The Johns Hopkins University
Applied Physics Laboratory
Geospace Remote Sensing

Coherent Radar Studies of the Ionosphere

by

Raymond A. Greenwald
The Johns Hopkins University
Applied Physics Laboratory

June 21, 1992

The Johns Hopkins University
Applied Physics Laboratory
Geospace Remote Sensing

Contents

- Characteristics of Coherent Scatter Cross-Sections
- Siting and Propagation Considerations
- Examples of Coherent Scatter Radars
- Plasma Instability Processes
- Spectral Characteristics of E- and F-Region Backscatter
- The Drift Motion of Ionospheric Irregularities
- Applications of Coherent Radars to Solar-Terrestrial Research
    - Convection Dynamics
    - Gravity Wave Excitation and Propagation
- SuperDARN

The Johns Hopkins University
Applied Physics Laboratory
Geospace Remote Sensing

Incoherent Scatter Cross-Section

$$\sigma_B = 4 \Pi r_e^2 N / (1+T_e / T_i)$$

Where:

N:	**Electron density**
T_e:	**Electron Temperature**
T_i:	**Ion Temperature**
r_e:	**Classical radius of electron**

SENSITIVITY DEPENDENCE FOR ASPECT RATIO (70) IRREGULARITIES

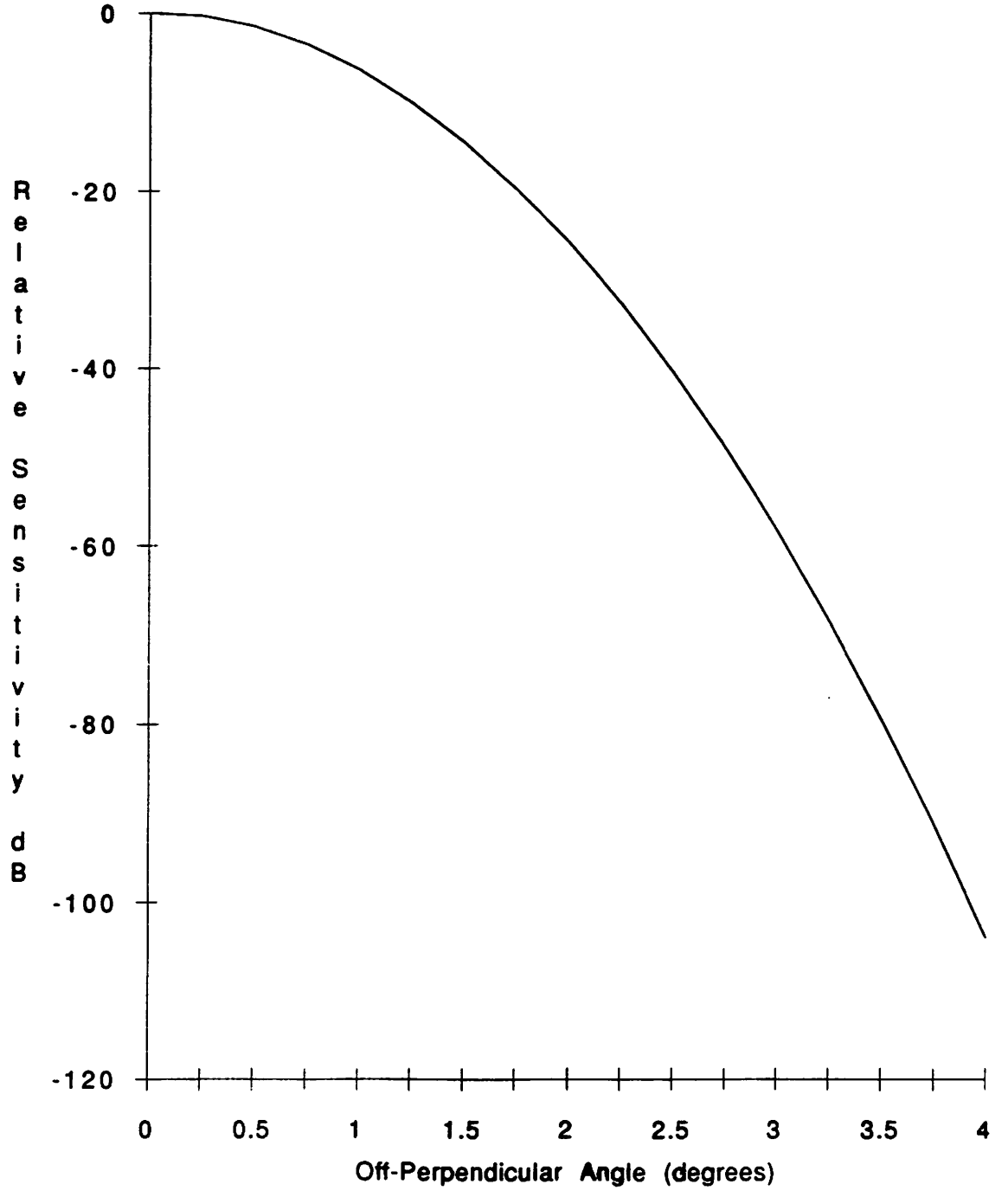

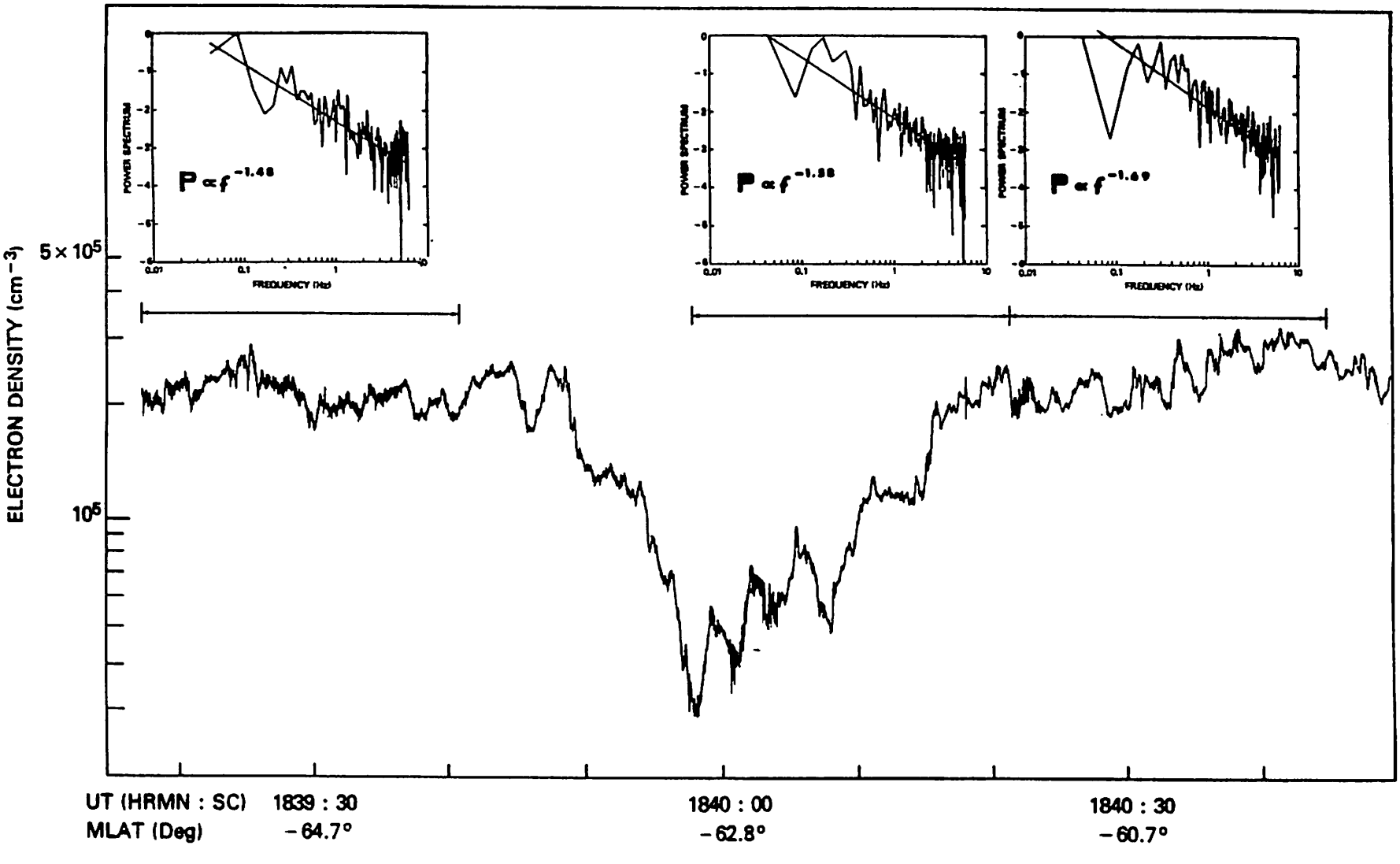

FIGURE 2. An expanded time-scale plot of electron density irregularities in the diffuse aurora of Figure 1. The power spectra indicate the frequency dependence of the least-squares power law. Frequency f is directly proportional to wave-number k, assuming the irregularities are spatial structures.

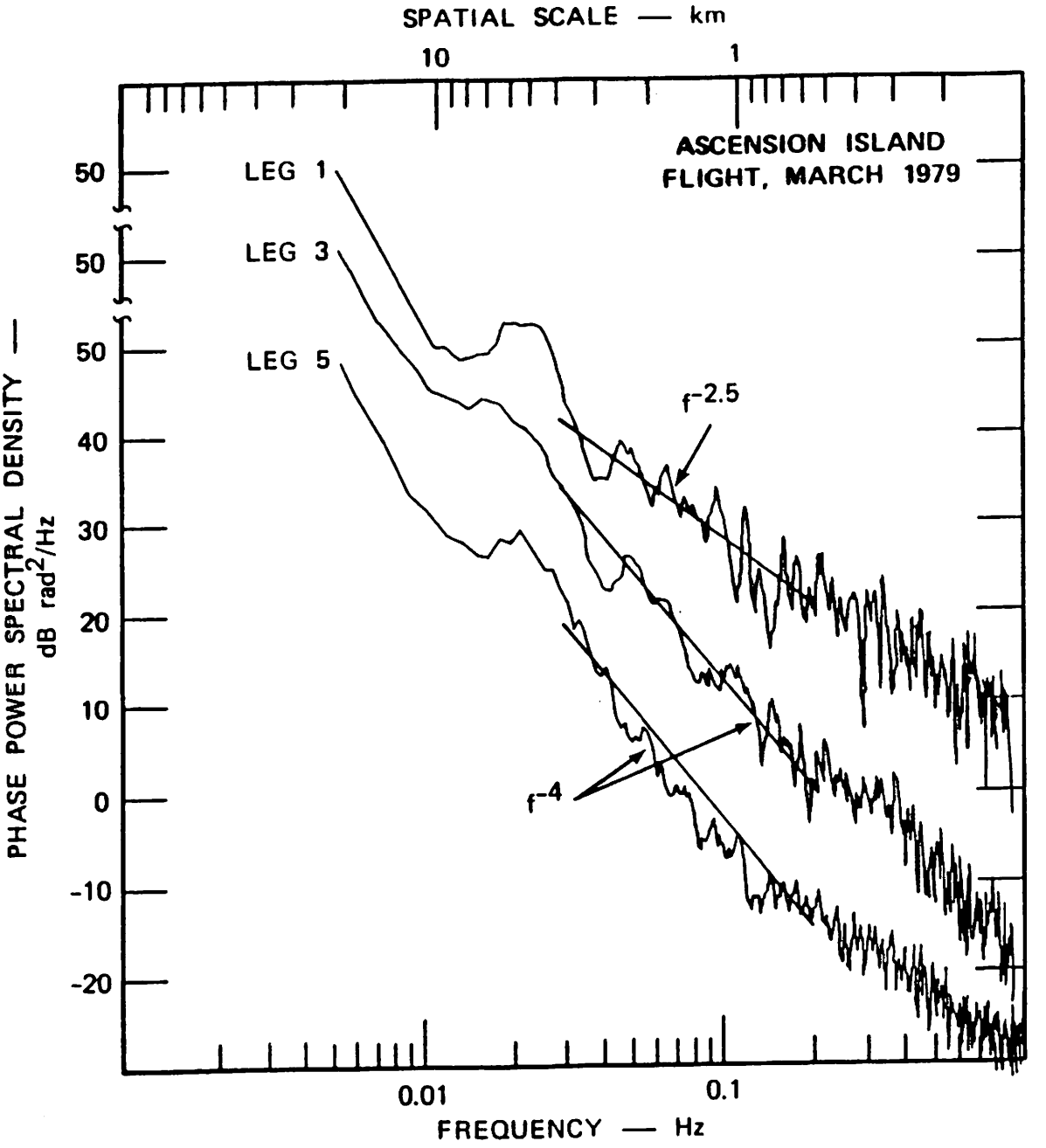

FIGURE IV.A.5 PHASE POWER SPECTRA FOR THE BUBBLE

The Johns Hopkins University
Applied Physics Laboratory
Geospace Remote Sensing

Comparison of Coherent Scatter and Incoherent Scatter Cross-Sections

For n = 3,

$$P_3(2k,0,0) \Rightarrow \Pi^{3/2}\alpha / 4\lambda_0 k^4$$

and

$$\sigma_c/\sigma_{inc} = \langle\Delta N^2\rangle(1+T_e/T_i)\,\Pi^{1/2}\,\alpha / (16\,N\,\lambda_0 k^4)$$

Assume

$\lambda_0 = 10$ km

$k = \Pi / 10$ (15 MHz)

$a = 70$

$N = 5 \times 10^5$

$\langle\Delta N^2\rangle^{1/2} / N = 10\%$

$T_e = T_i$

Then: $\sigma_c/\sigma_{inc} \approx 160$

MEASUREMENT OF FLUCTUATION LEVEL

BACKSCATTER CROSS SECTION (BOOKER, 1956)

$$\sigma_B = r_e^2 \langle \Delta N^2 \rangle P_3 (k_1, k_2, k_3)$$

WHERE $r_e = 2.8 \times 10^{-15}$m = CLASSICAL ELECTRON RADIUS

$\langle \Delta N^2 \rangle$ = MEAN SQUARE ELECTRON DENSITY FLUCTUATION LEVEL

$P_3(k_1, k_2, k_3)$ = 3D SPATIAL POWER SPECTRUM

ASSUME

$$P_3(k_\perp, 0, k_\parallel) = \frac{A_\perp e^{-(\lambda_0 \alpha k_\parallel)^2/(1 + \lambda_0^2 k_\perp^2)}}{(1 + \lambda_0^2 k_\perp^2)^{n + \frac{1}{2}}}$$

WHERE λ_0 = OUTER SCALE LENGTH OF TURBULENCE

α = ASPECT RATIO OF IRREGULARITIES

$n > 1$

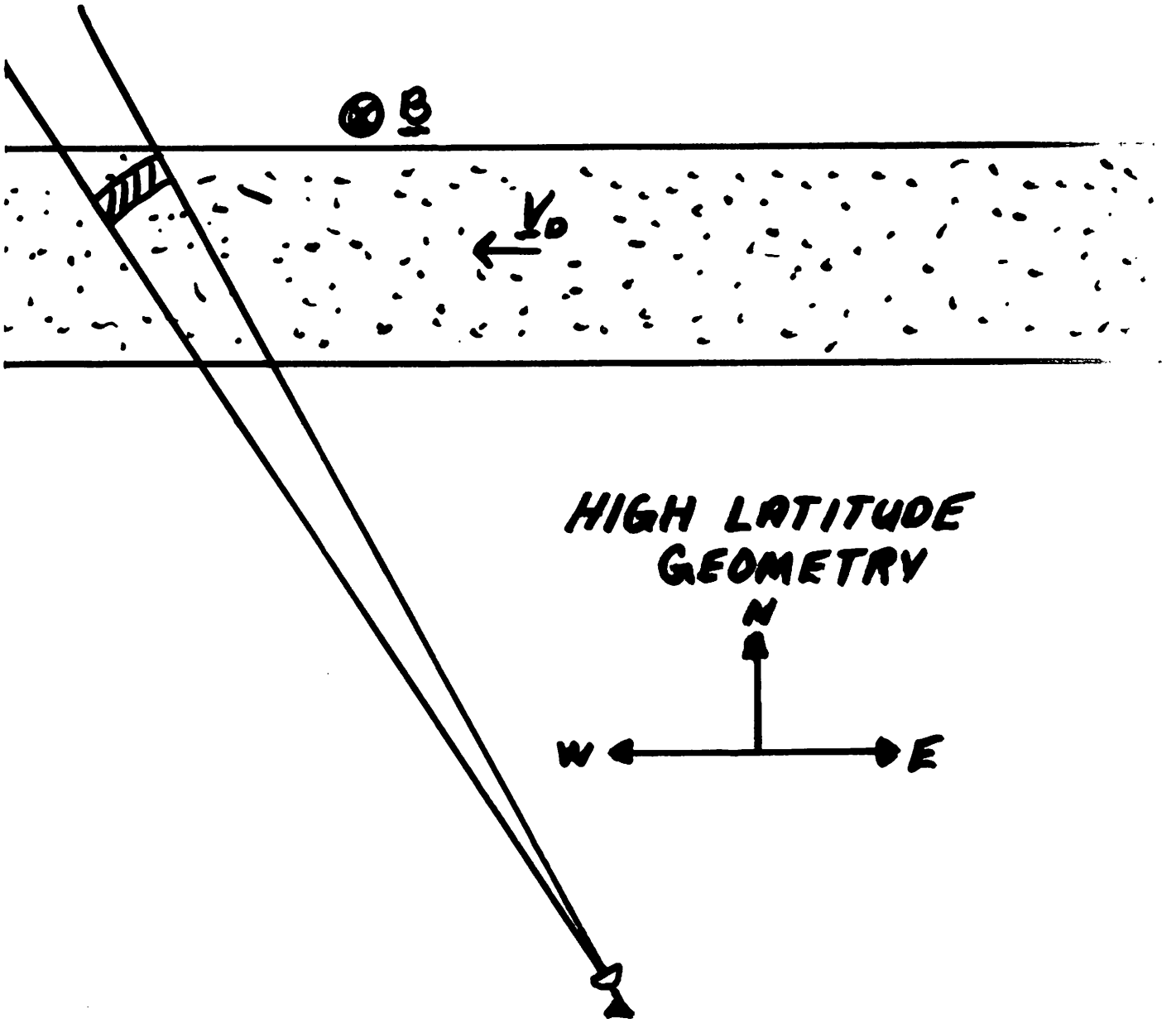

EQUATORIAL GEOMETRY

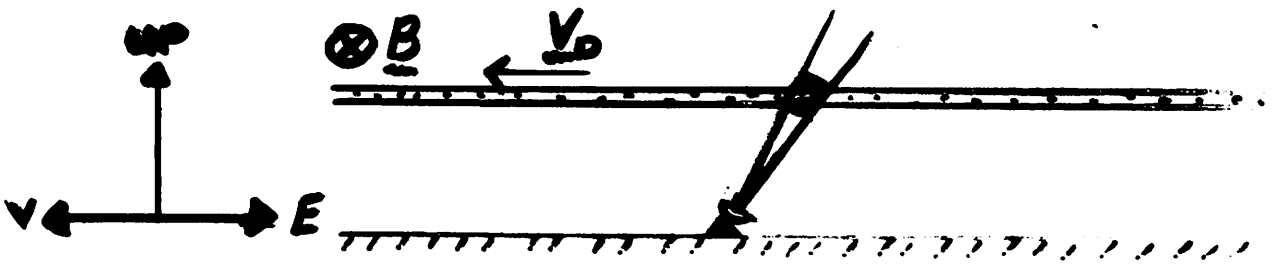

HF PROPAGATION IN A HORIZONTALLY-STRATIFIED IONOSPHERE

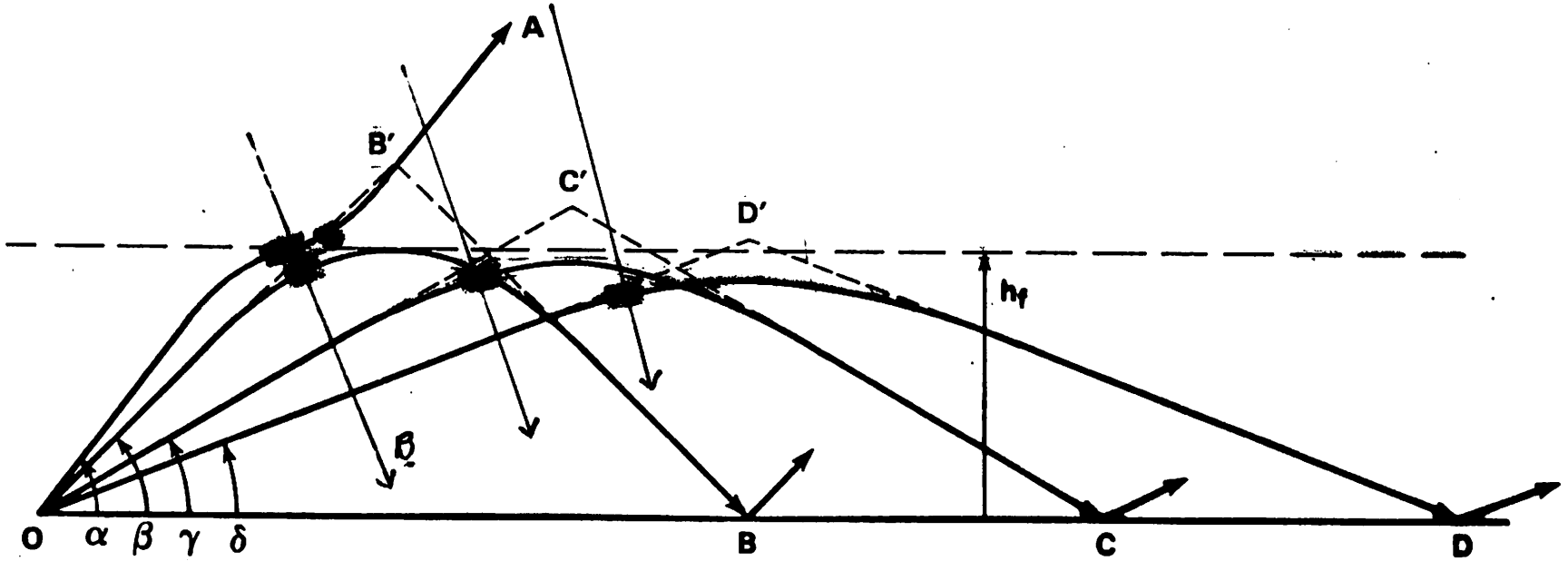

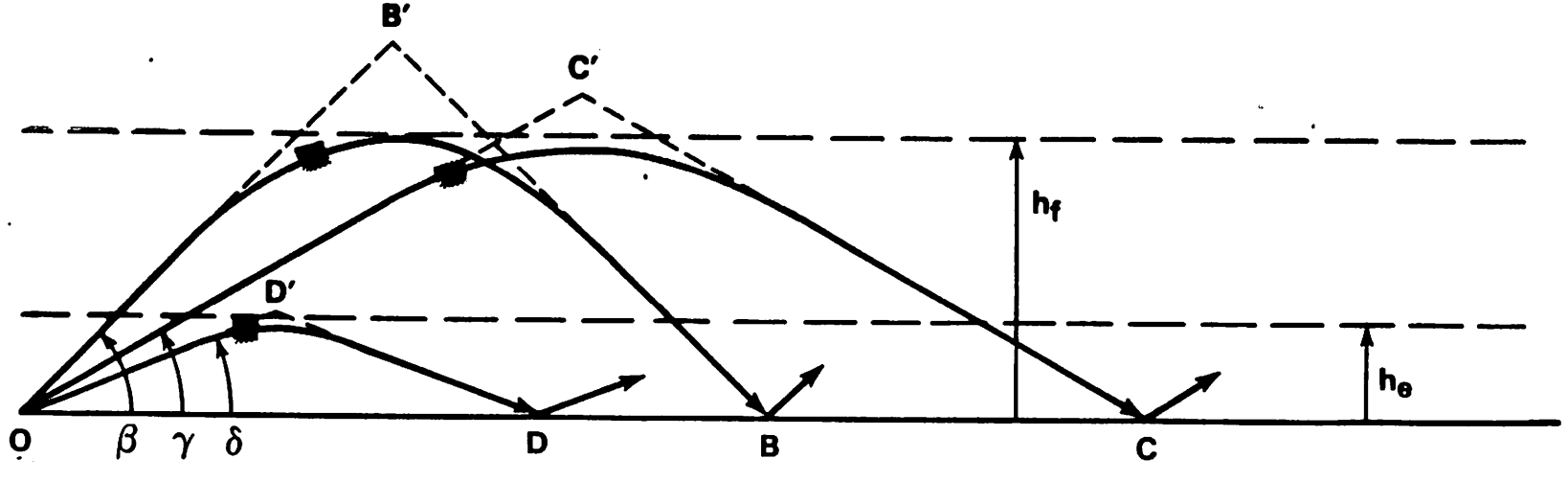

The Johns Hopkins University
Applied Physics Laboratory
Geospace Remote Sensing

Drift of F-Region Irregularities

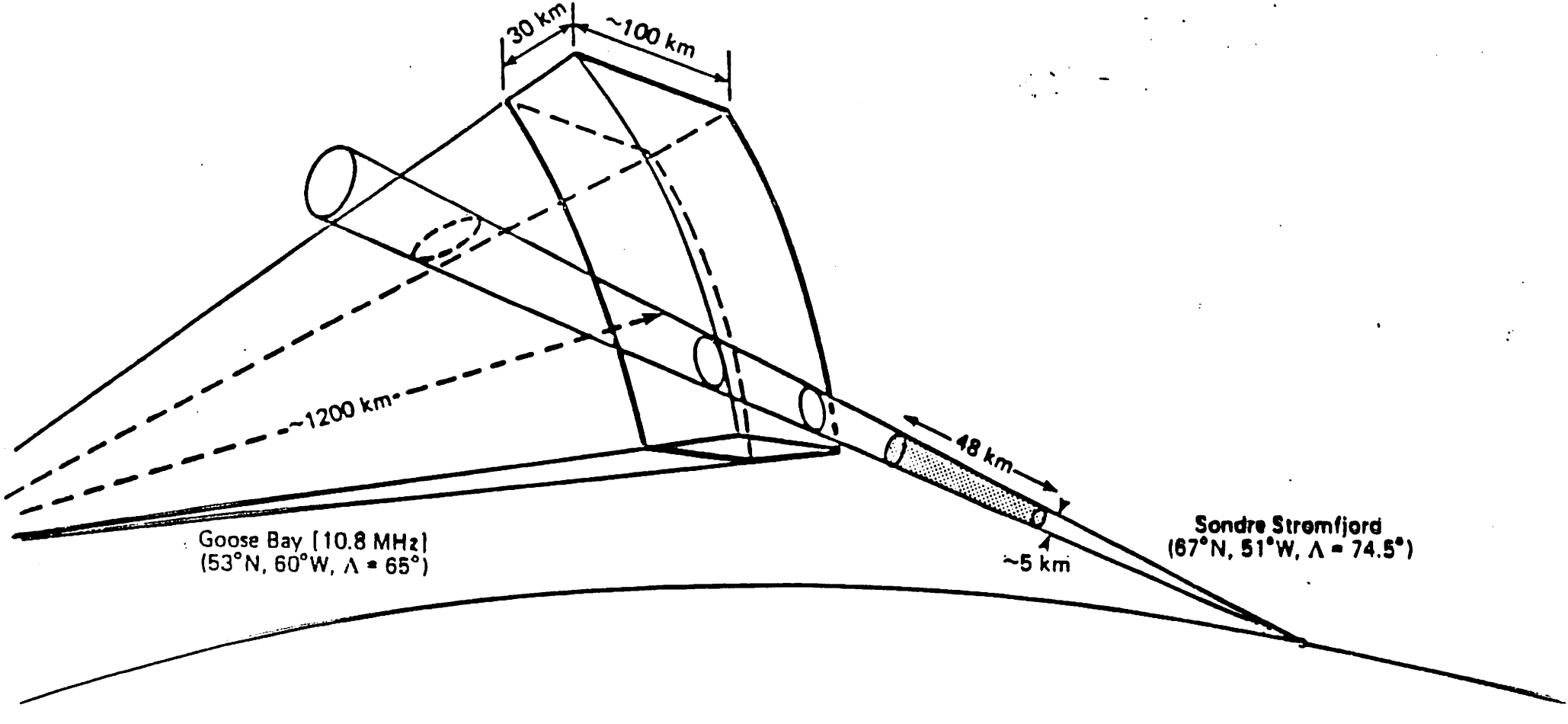
30 km
~100 km
~1200 km
48 km
~5 km
Goose Bay [10.8 MHz]
(53°N, 60°W, Λ = 65°)
Sondre Stromfjord
(67°N, 51°W, Λ = 74.5°)

Fig. 1

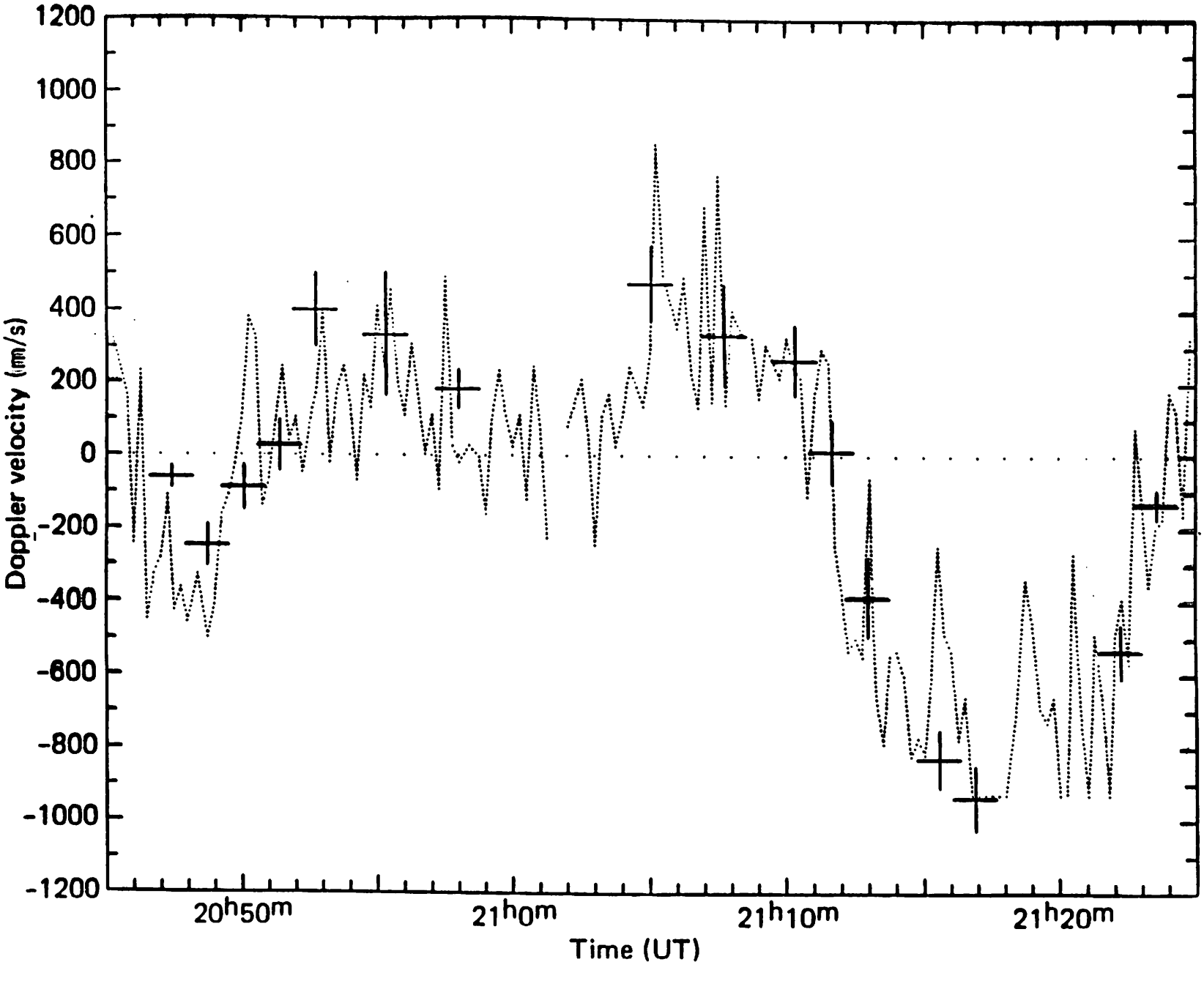
1200
1000
800
600
400
200
0
-200
-400
-600
-800
-1000
-1200
Doppler velocity (m/s)
20h50m
21h0m
21h10m
21h20m
Time (UT)

The Johns Hopkins University
Applied Physics Laboratory
Geospace Remote Sensing

Plasma Instabilities

The Johns Hopkins University
Applied Physics Laboratory
Geospace Remote Sensing

Categories of Plasma Instability

Source of Free Energy	Type of Instability
Streaming of one particle species relative to another	Streaming Instability
Gradient in plasma density or temperature plus external force	Gradient Instability
Gradient in plasma density or temperature without external force	Universal Instability
Non-Maxwellian particle distribution	Kinetic Instability

E-REGION GRADIENT-DRIFT INSTABILITY (DUE TO ELECTRON HALL DRIFT)

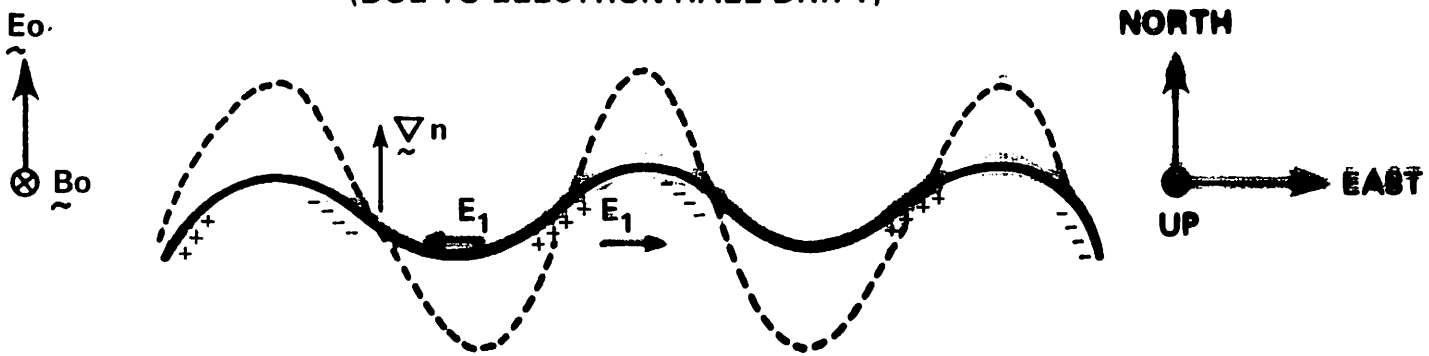

F-REGION GRADIENT-DRIFT INSTABILITY (DUE TO ION PEDERSEN DRIFT)

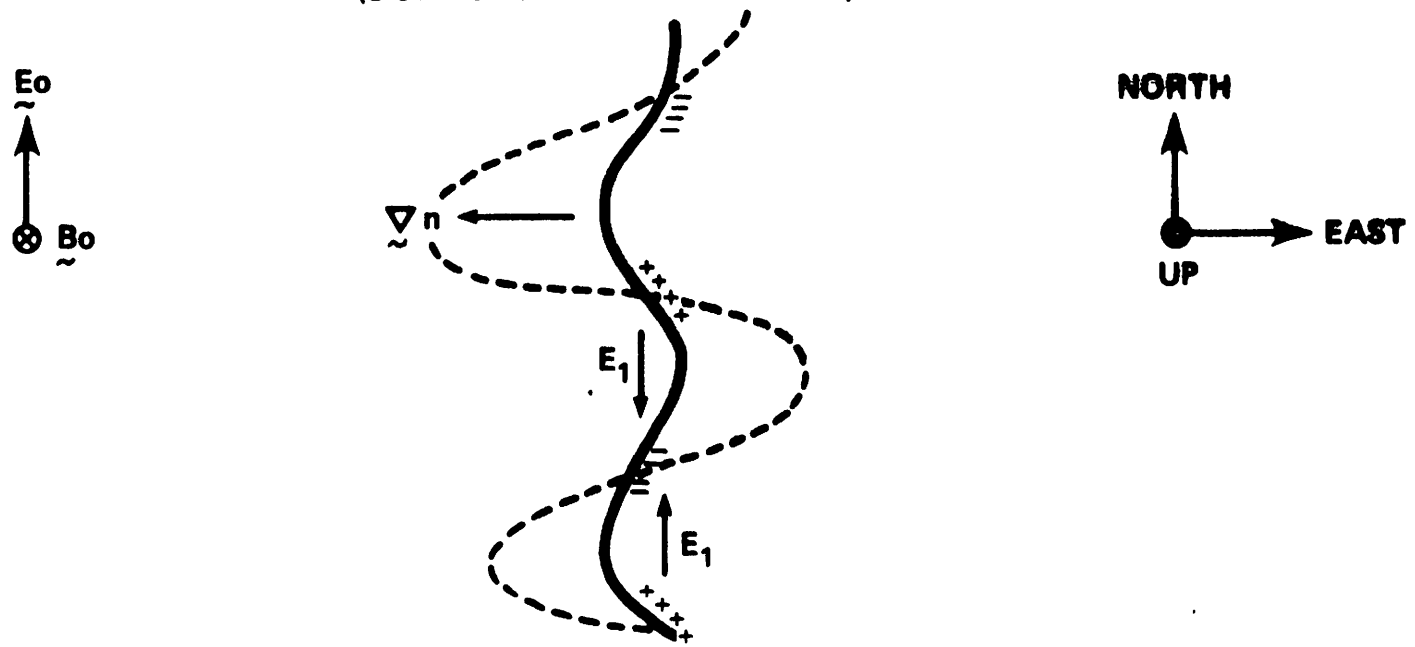

CASE 2. GRADIENT DRIFT INSTABILITY

$k_\parallel = 0 \quad v_d \ll c_s \quad L_N \neq \infty \quad \psi \ll 1$

$$\Gamma = \frac{k \cdot v_d \nu_i}{k L_N \Omega_i} - \frac{\psi}{\nu_i} k^2 c_s^2$$

$$\omega_r = \underset{\sim}{k} \cdot \underset{\sim}{v_d}$$

CASE 3. MODIFIED TWO-STREAM INSTABILITY

$k_\parallel \neq 0 \,, L_N = \infty \,, \psi > 1 \,, \quad \underset{\sim}{v_d} = \{ v_{d\parallel}, v_{d\perp} \}$

$$\frac{\nu_i}{\Omega_i} \gtrsim 1$$

$$\Gamma \simeq \frac{1}{\nu_i} \left[(\underset{\sim}{k} \cdot \underset{\sim}{v_d} / \psi)^2 - k^2 c_s^2 \right]$$

$$\omega_r \simeq \underset{\sim}{k} \cdot \underset{\sim}{v_d} / \psi$$

THRESHOLD: $\omega_r / k = c_s$

CASE 4. ELECTROSTATIC ION CYCLOTRON INSTABILITY

$k_\parallel \neq 0 \,, L_N = \infty \,, \psi > 1 \,, v_d = \{ v_{d\parallel}, v_{d\perp} \}$

$$\frac{\nu_i}{\Omega_i} \ll 1$$

THRESHOLD: $\omega_r / k_\perp = \left(\Omega_i^2 / k^2 + c_s^2 \right)^{1/2}$

E AND F_1 REGION PLASMA STREAMING INSTABILITIES

$\underset{\sim}{C_s}$ = ACOUSTIC VELOCITY

$\underset{\sim}{V_d}$ = RELATIVE ELECTRON-ION DRIFT $\{V_{d\perp}, V_{d\parallel}\}$

L_N = DENSITY GRADIENT SCALE LENGTH

$$\psi = \left(\frac{\nu_i}{\Omega_i}\right)\left(1 + \Omega_e^2 k_\perp^2 / \nu_e^2 k^2\right)$$

$$k_\parallel = 0 \Rightarrow \psi = \left(\frac{\nu_e \nu_i}{\Omega_e \Omega_i}\right) \ll 1$$

$$k_\parallel \neq 0 \Rightarrow \psi = \left(\frac{\nu_i \Omega_e}{\nu_e \Omega_i}\right)\frac{k_\parallel^2}{k^2} > 1$$

CASE 1. CROSS FIELD TWO-STREAM INSTABILITY

$k_\parallel = 0 \quad L_N = \infty \quad \psi \ll 1$

$$\Gamma = \frac{\psi}{\nu_i} k^2 (V_d^2 - C_s^2)$$

$$\omega_r = \underset{\sim}{k} \cdot \underset{\sim}{V_d}$$

THRESHOLD: $\omega_r / k = C_s$

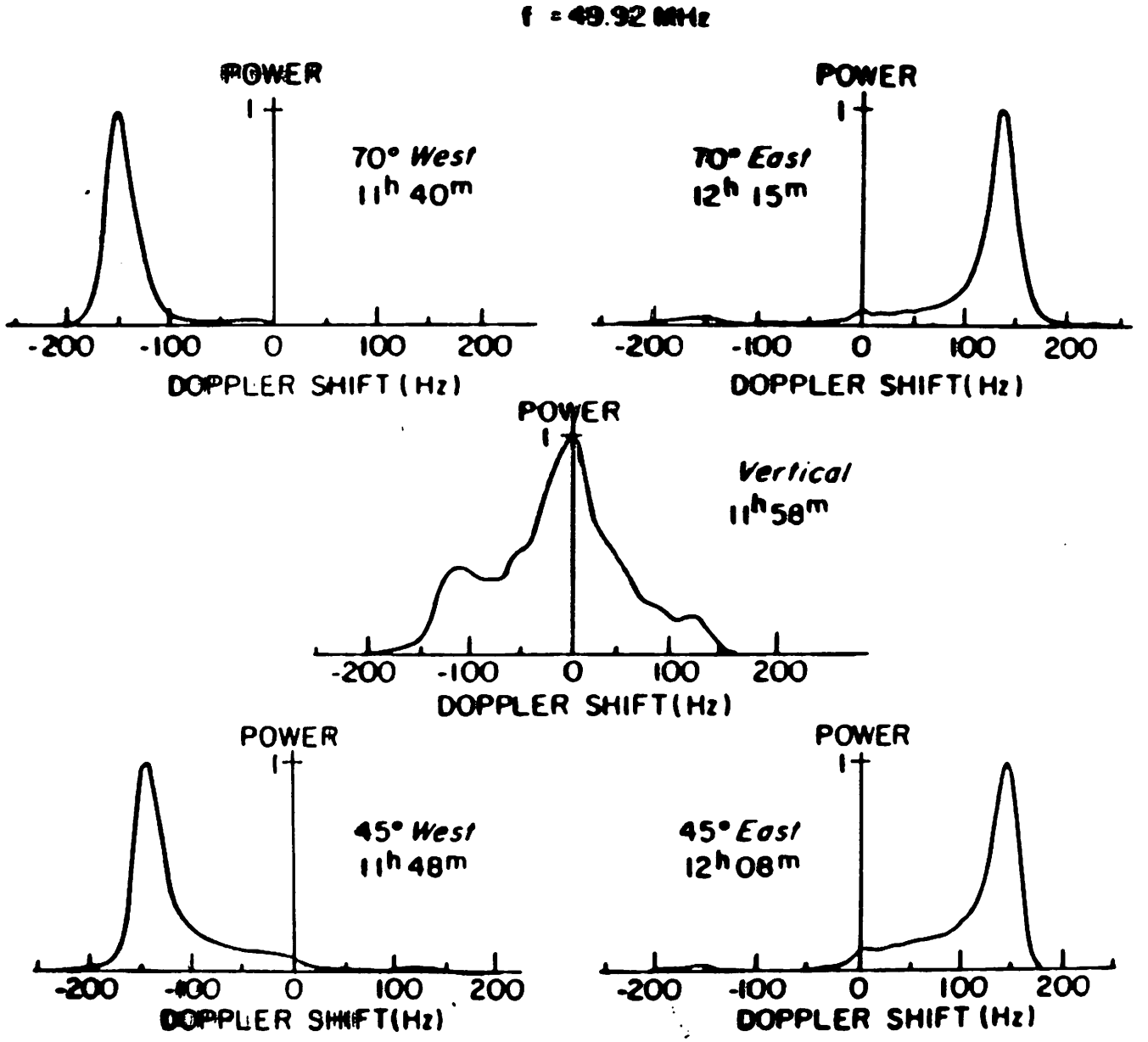

Fig. 4.20. Series of Doppler spectra from the equatorial electrojet irregularities at different elevation angles obtained at Jicamarca during a period of relatively strong scattering. The spectra are normalized to a fixed peak value. [After Cohen and Bowles (1967). Reproduced with permission of the American Geophysical Union.]

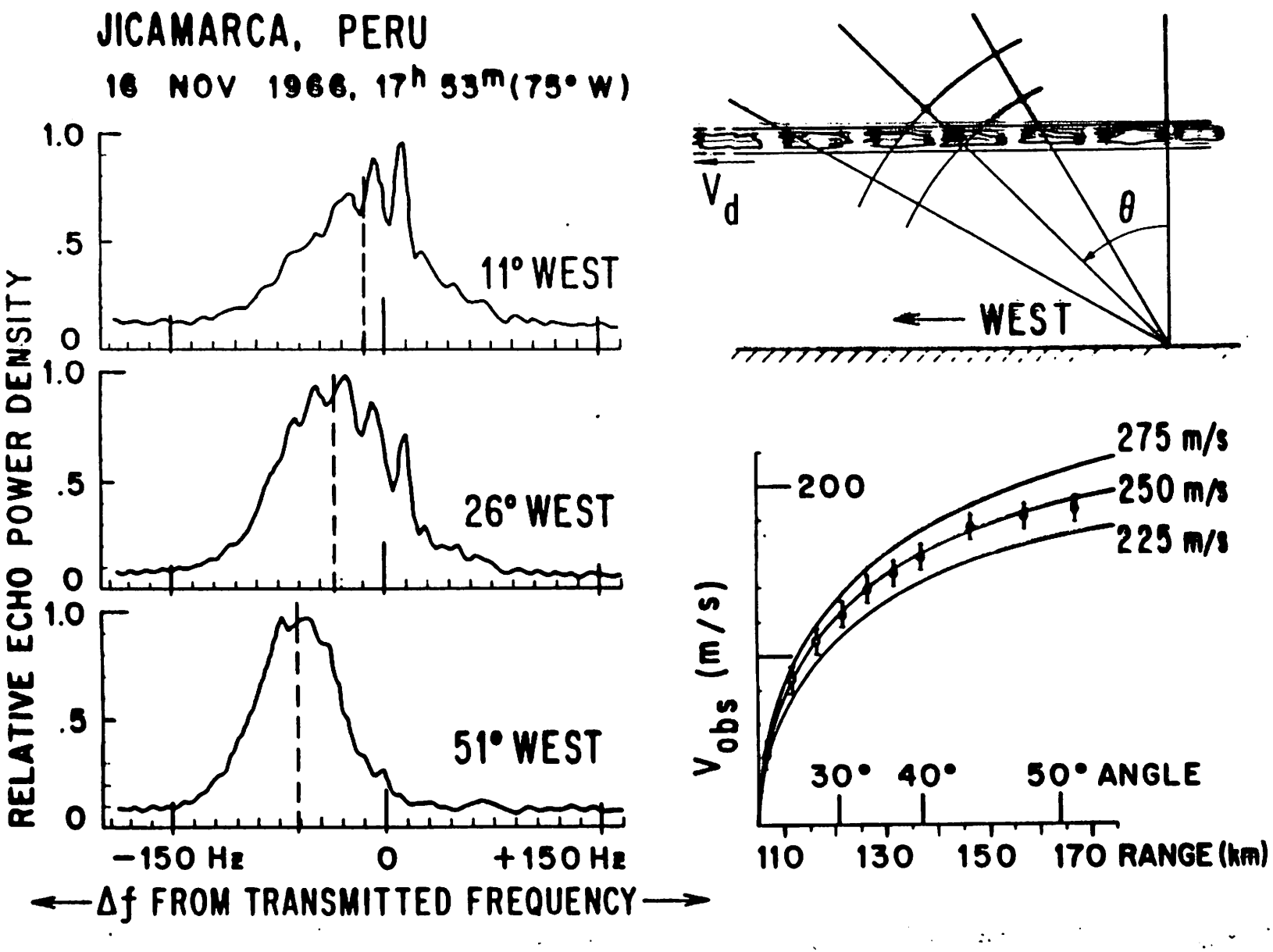
JICAMARCA, PERU
16 NOV 1966, 17h 53m (75° W)
1.0
.5
0
11° WEST
26° WEST
51° WEST
RELATIVE ECHO POWER DENSITY
−150 Hz
0
+150 Hz
← Δf FROM TRANSMITTED FREQUENCY →
V_d
θ
WEST
275 m/s
250 m/s
225 m/s
200
V_{obs} (m/s)
30°
40°
50° ANGLE
110
130
150
170 RANGE (km)

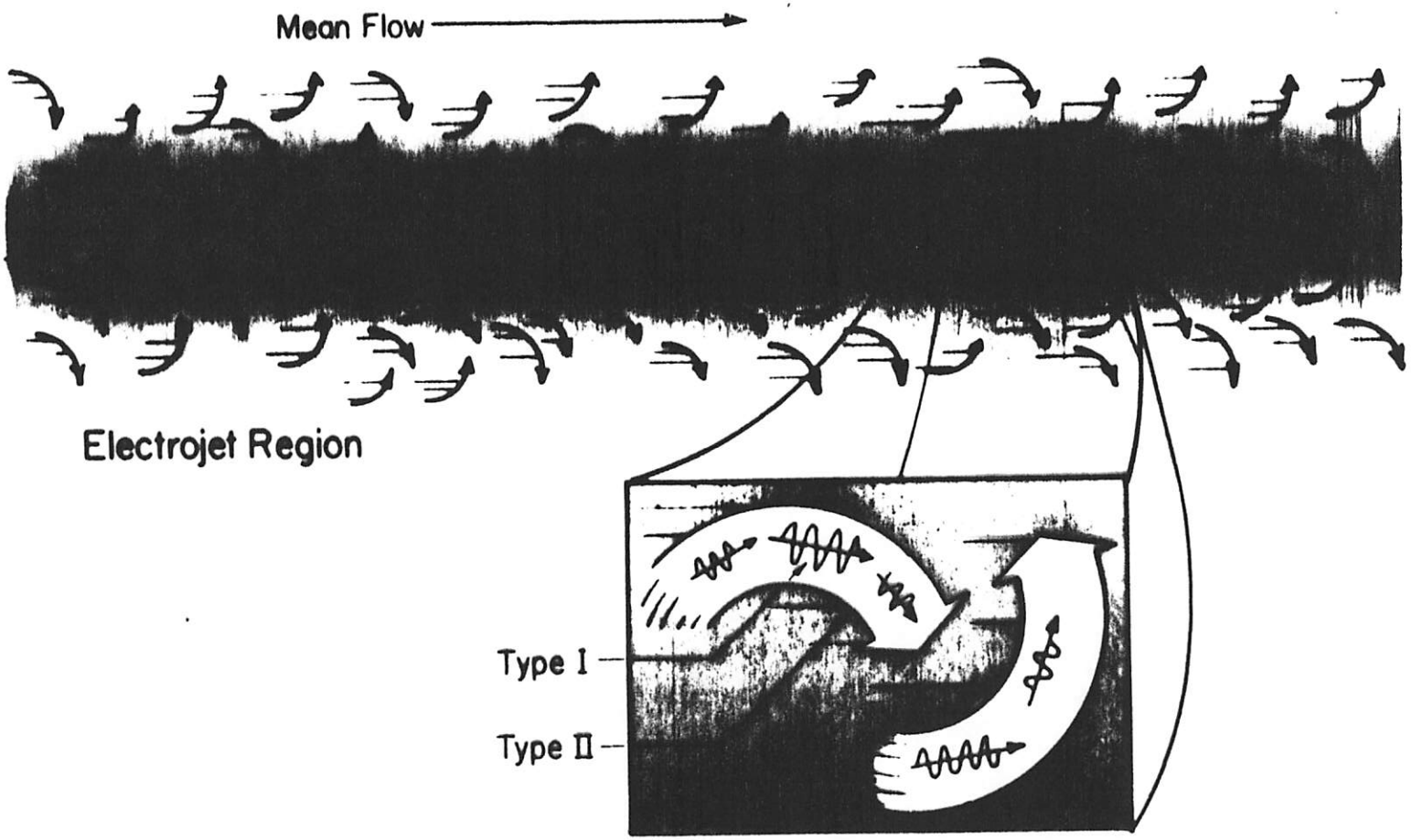
Mean Flow
Electrojet Region
Type I
Type II

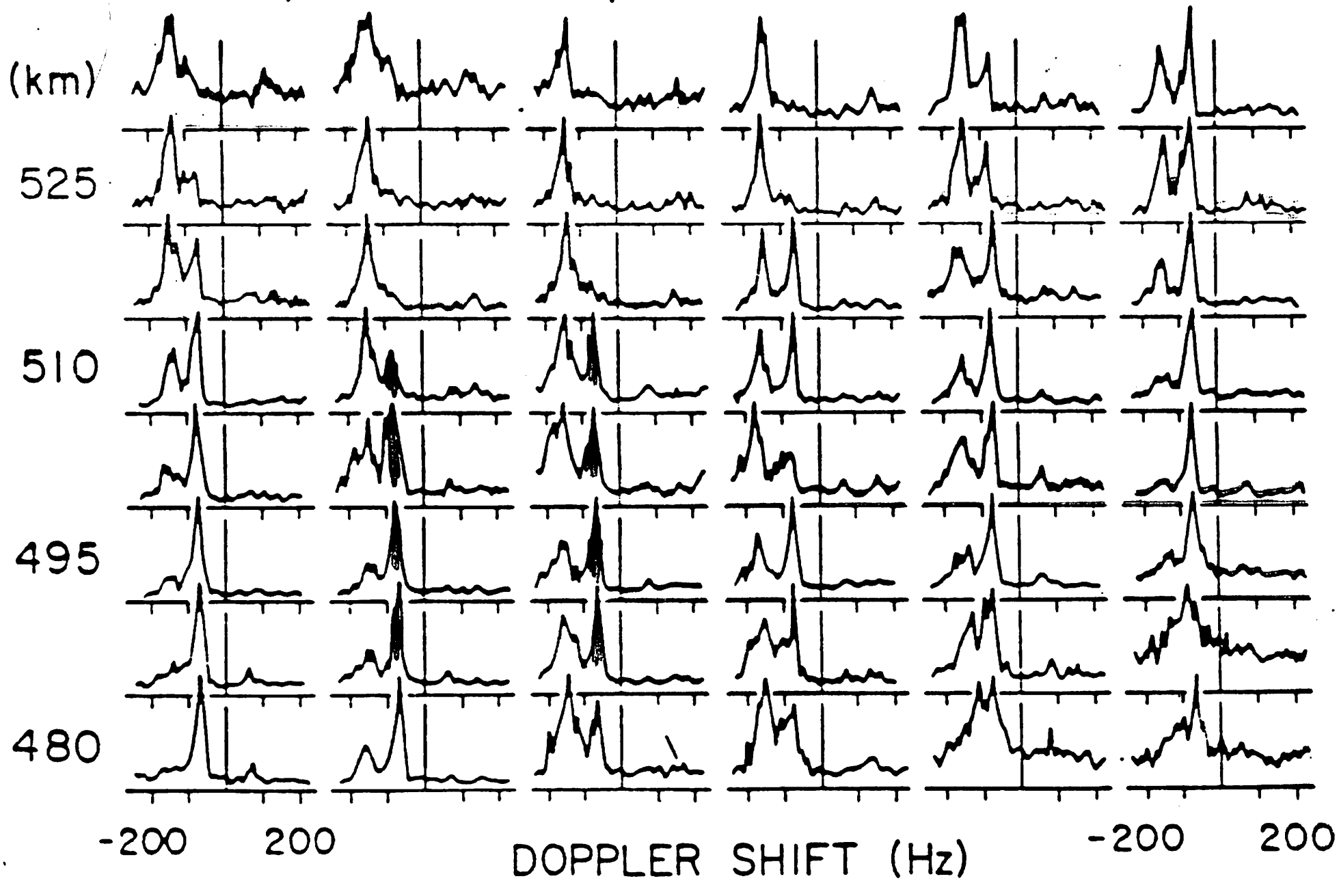
ITHACA, N.Y. APRIL 1, 1976 02:04:15-02:04:28 LT
(km)
525
510
495
480
-200
200
-200
200
DOPPLER SHIFT (Hz)

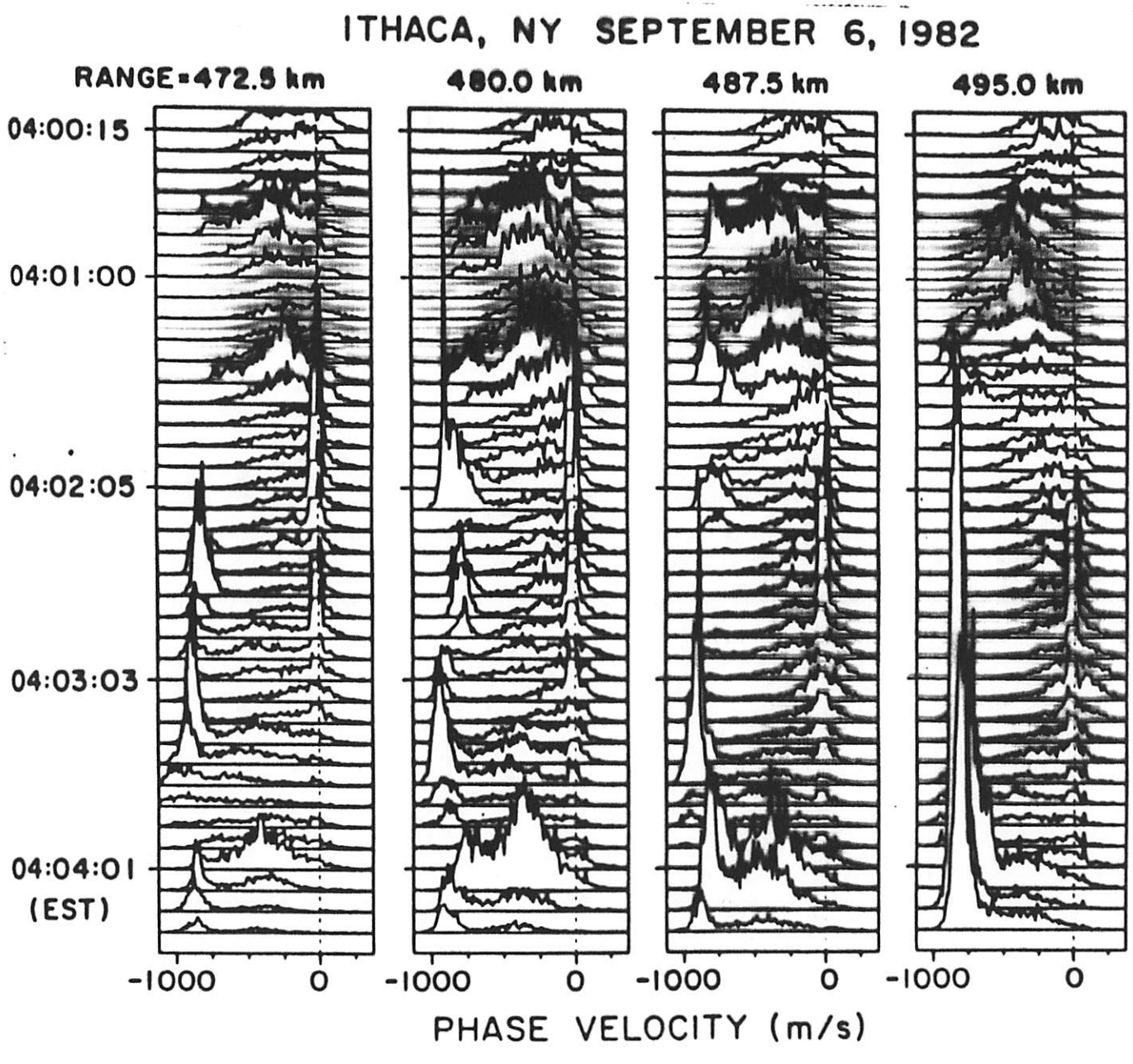
ITHACA, NY SEPTEMBER 6, 1982
RANGE=472.5 km
480.0 km
487.5 km
495.0 km
04:00:15
04:01:00
04:02:05
04:03:03
04:04:01
(EST)
-1000
0
-1000
0
-1000
0
-1000
0
PHASE VELOCITY (m/s)

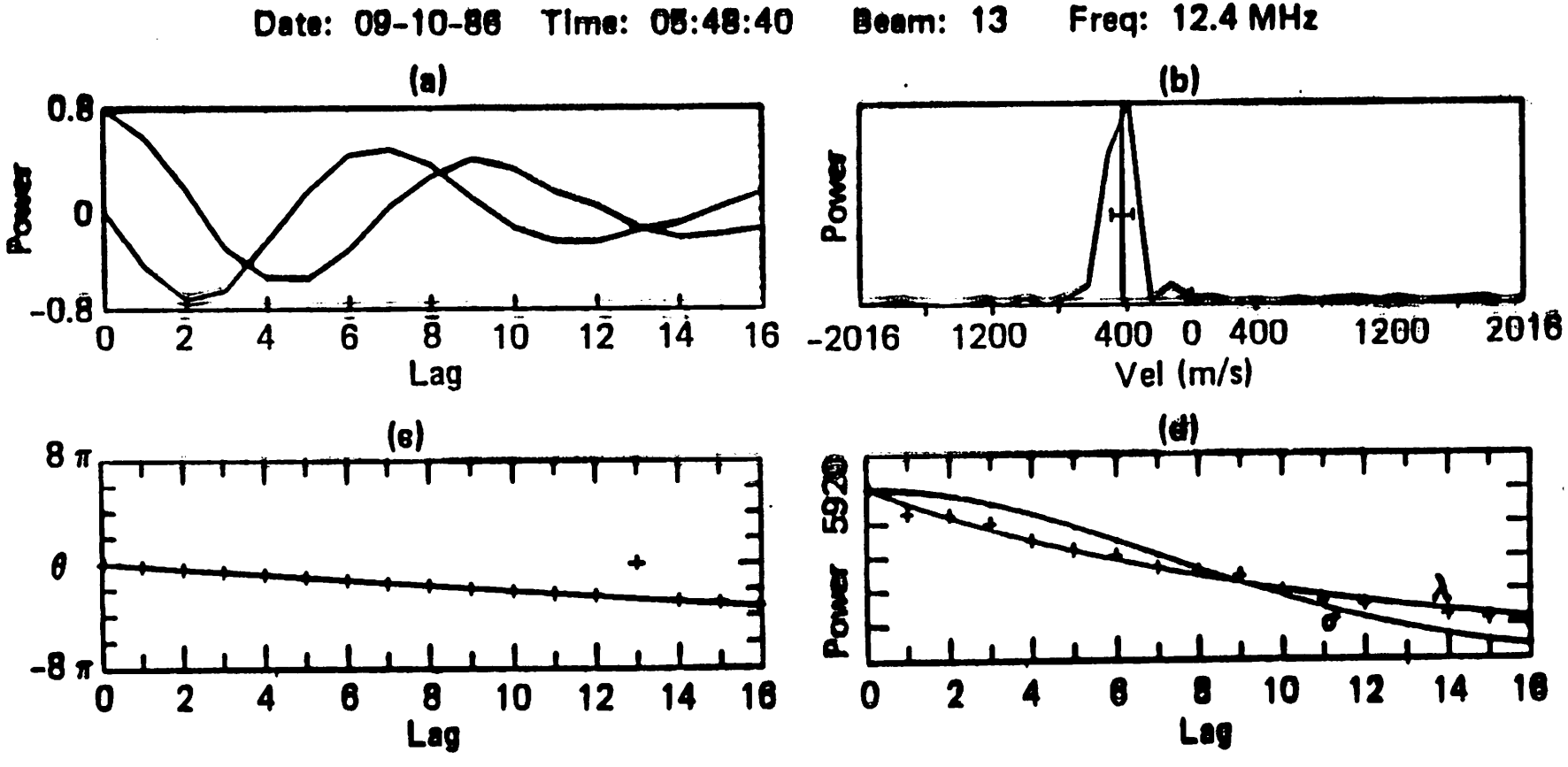

Figure 5. Stages in the processing of a sample of HF radar data. (a) Real and imaginary parts of an ACF. (b) Doppler spectrum obtained by Fourier transformation of the ACF. (c) Phase angle as a function of lag and its linear least-squares fit. (d) Power variation of the ACF as a function of lag and fits based on exponential λ and exponential $\sigma = \lambda^2$ as explained in the text. [*Reprinted from Villain et al.*, 1987]

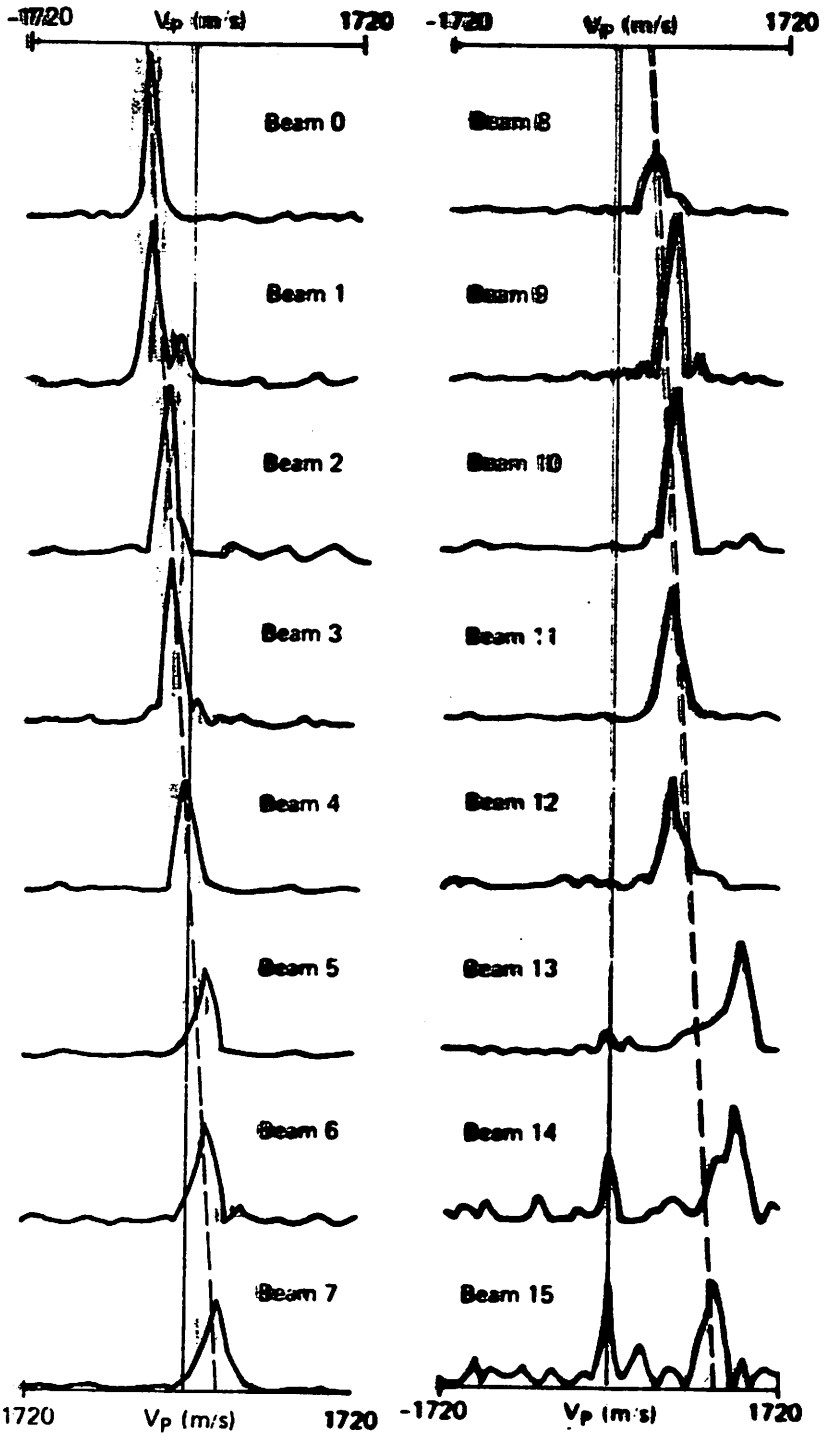

12 October 1983 2001:32 – 2002:52 UT
Frequency = 14.5 MHz Range = 1100 km

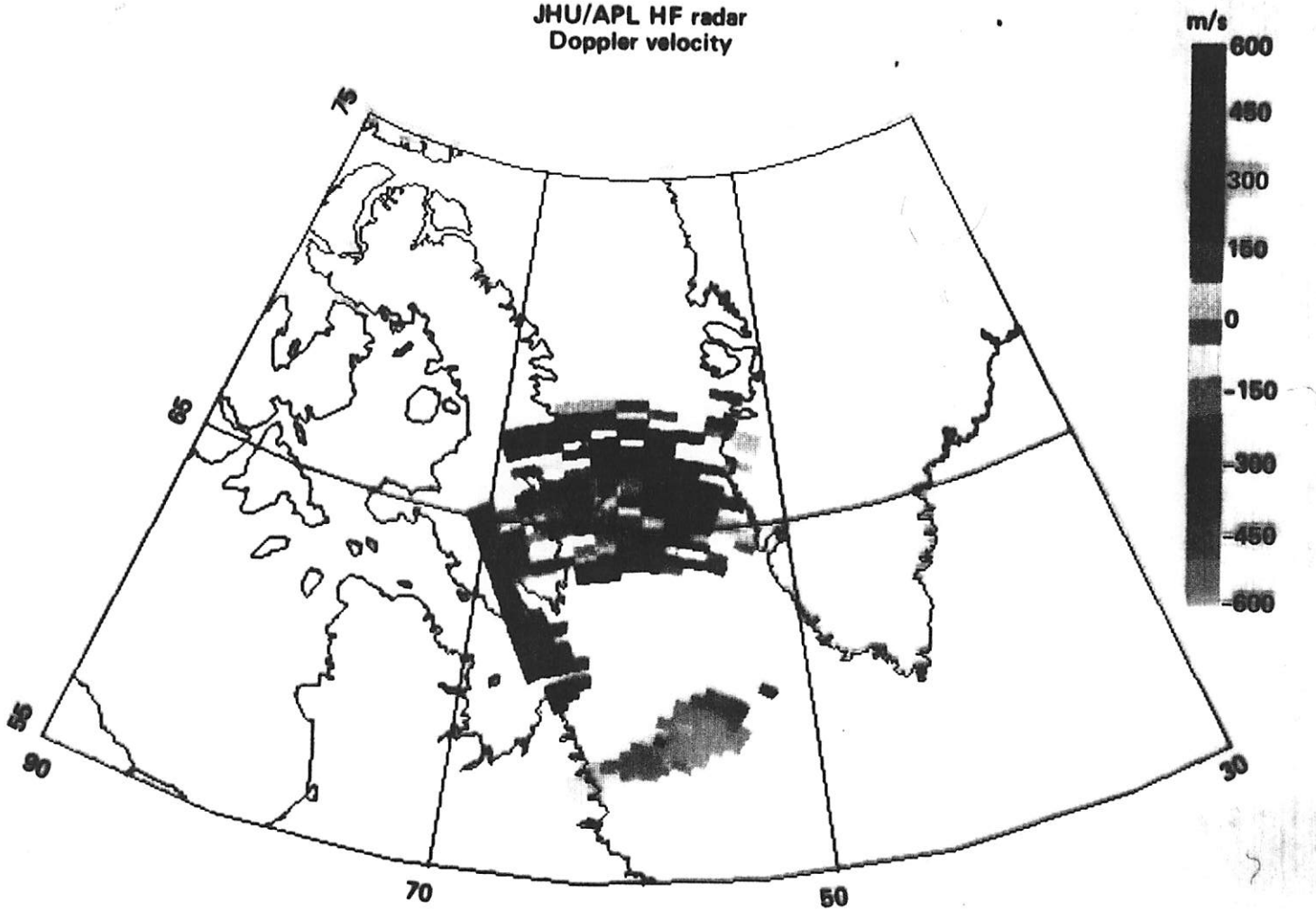
JHU/APL HF radar
Doppler velocity
m/s
600
450
300
150
0
-150
-300
-450
-600
75
65
55
90
70
50
30
Frequency: 12.3 MHz
Date: 9-10-86
Time: 05:51:35

Date: 09-10-86 Start time: 05:51:35 Freq: 12.4 MHz

Beam:	00	01	02	03	04	05	06	07	08	09	10	11	12	13	14	15
Range:	09	09	09	09	09	09	10	10	11	11	12	13	14	16	17	20

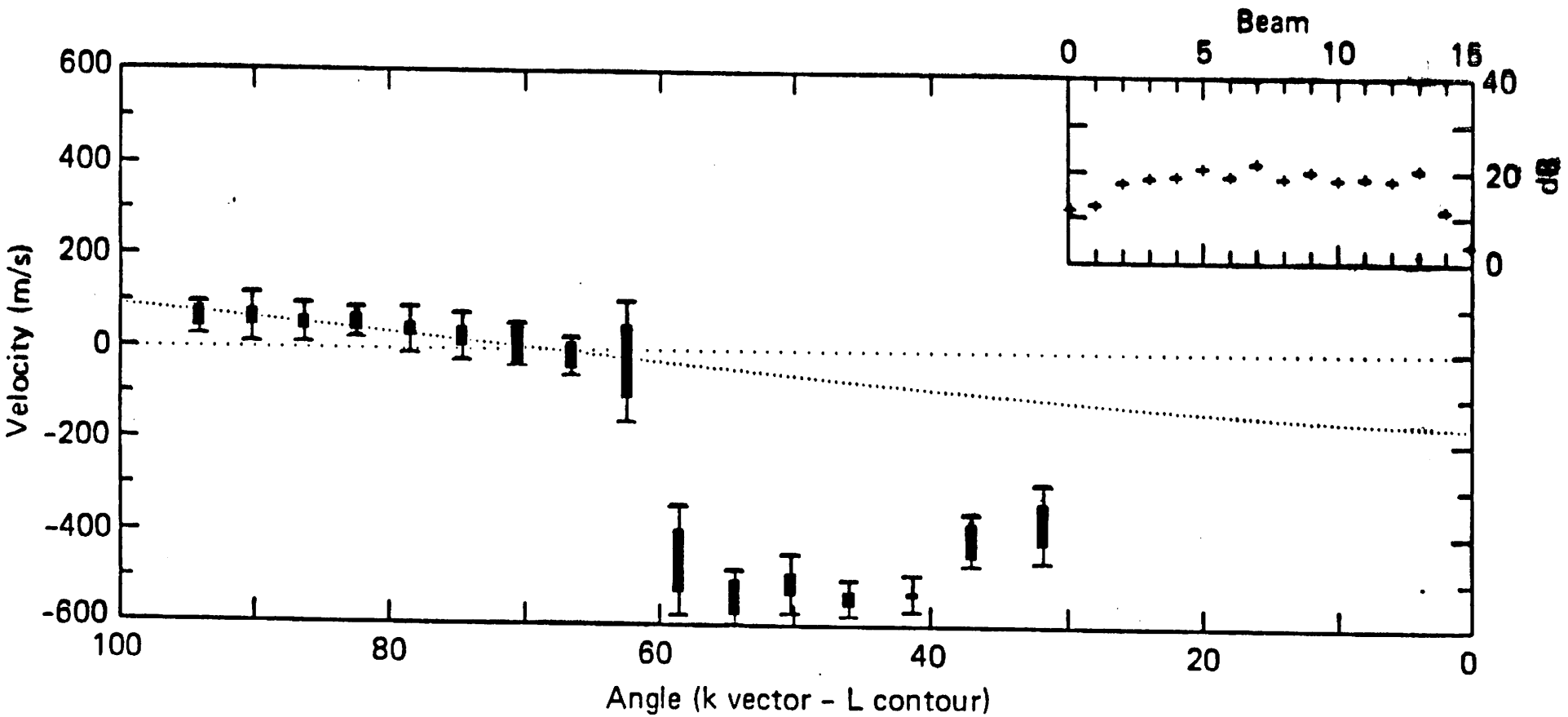

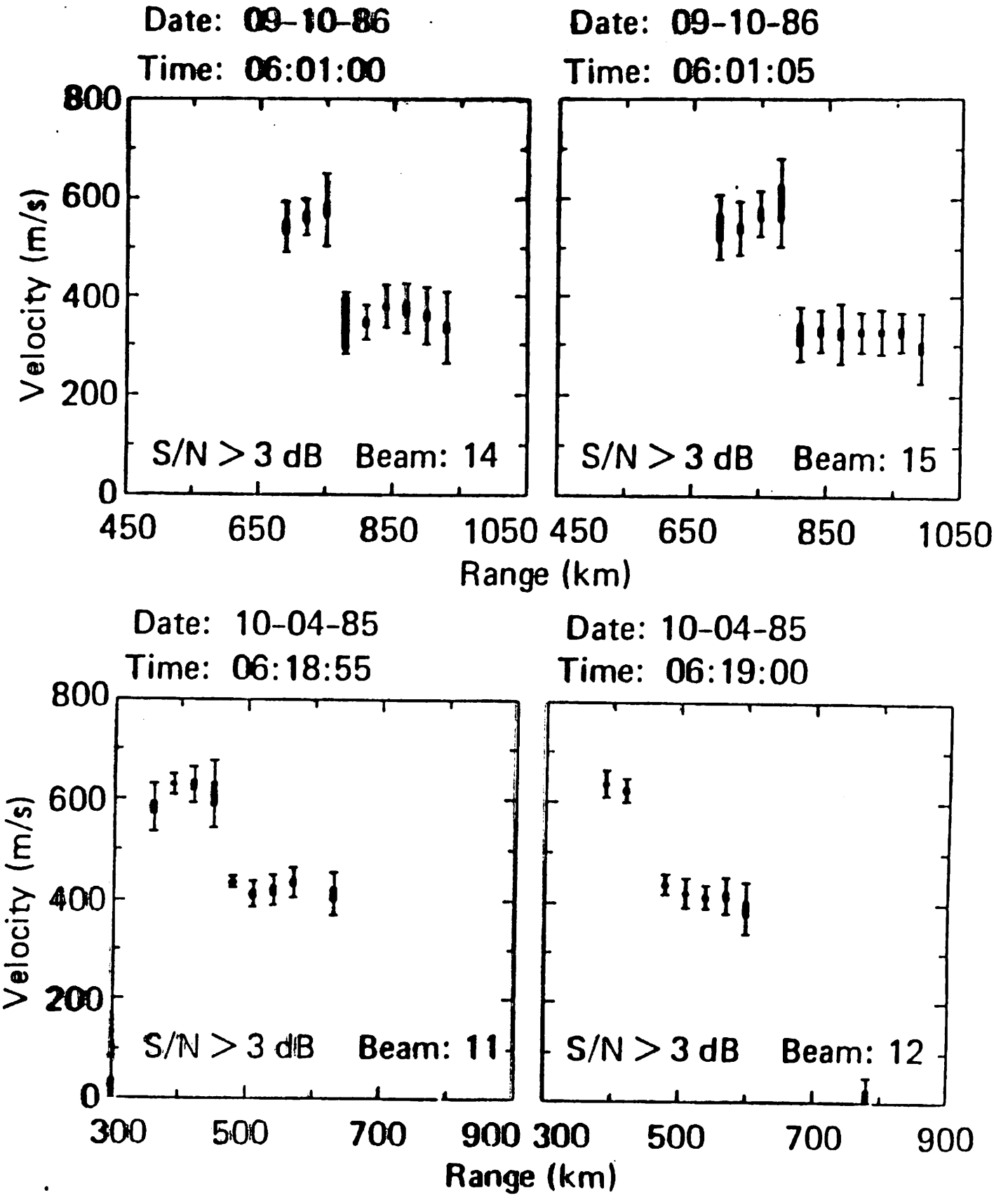
Date: 09-10-86
Time: 06:01:00
Date: 09-10-86
Time: 06:01:05
800
600
400
200
0
Velocity (m/s)
S/N > 3 dB Beam: 14
S/N > 3 dB Beam: 15
450
650
850
1050
Range (km)
Date: 10-04-85
Time: 06:18:55
Date: 10-04-85
Time: 06:19:00
800
600
400
200
0
Velocity (m/s)
S/N > 3 dB Beam: 11
S/N > 3 dB Beam: 12
300
500
700
900
Range (km)

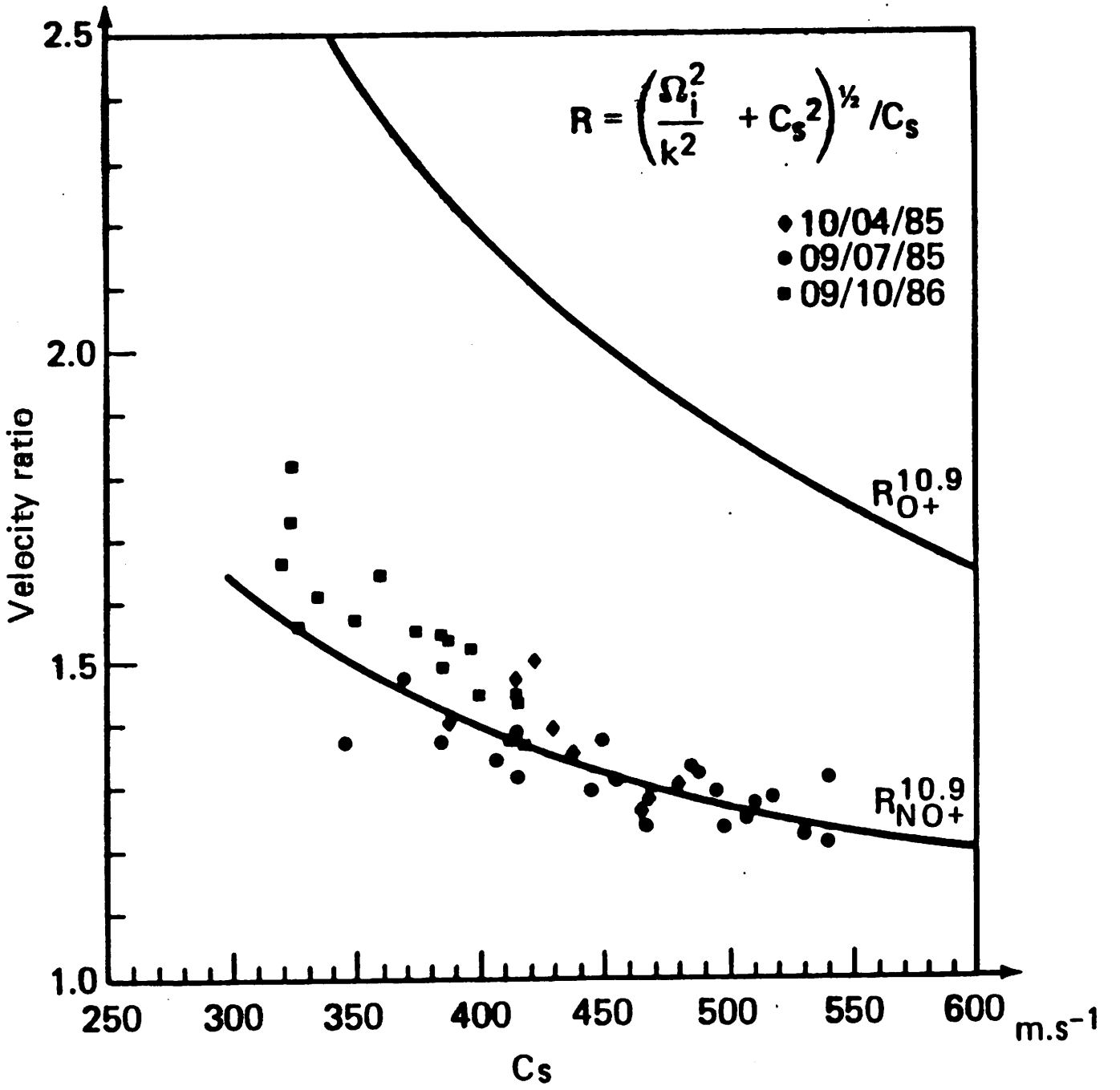
2.5
2.0
1.5
1.0
Velocity ratio
$R = \left(\frac{\Omega_i^2}{k^2} + C_s^2\right)^{1/2} / C_s$
• 10/04/85
• 09/07/85
▪ 09/10/86
$R_{O^+}^{10.9}$
$R_{NO^+}^{10.9}$
250
300
350
400
450
500
550
600
m.s-1
Cs

The Johns Hopkins University
Applied Physics Laboratory
Geospace Remote Sensing

DAYSIDE CONVECTION

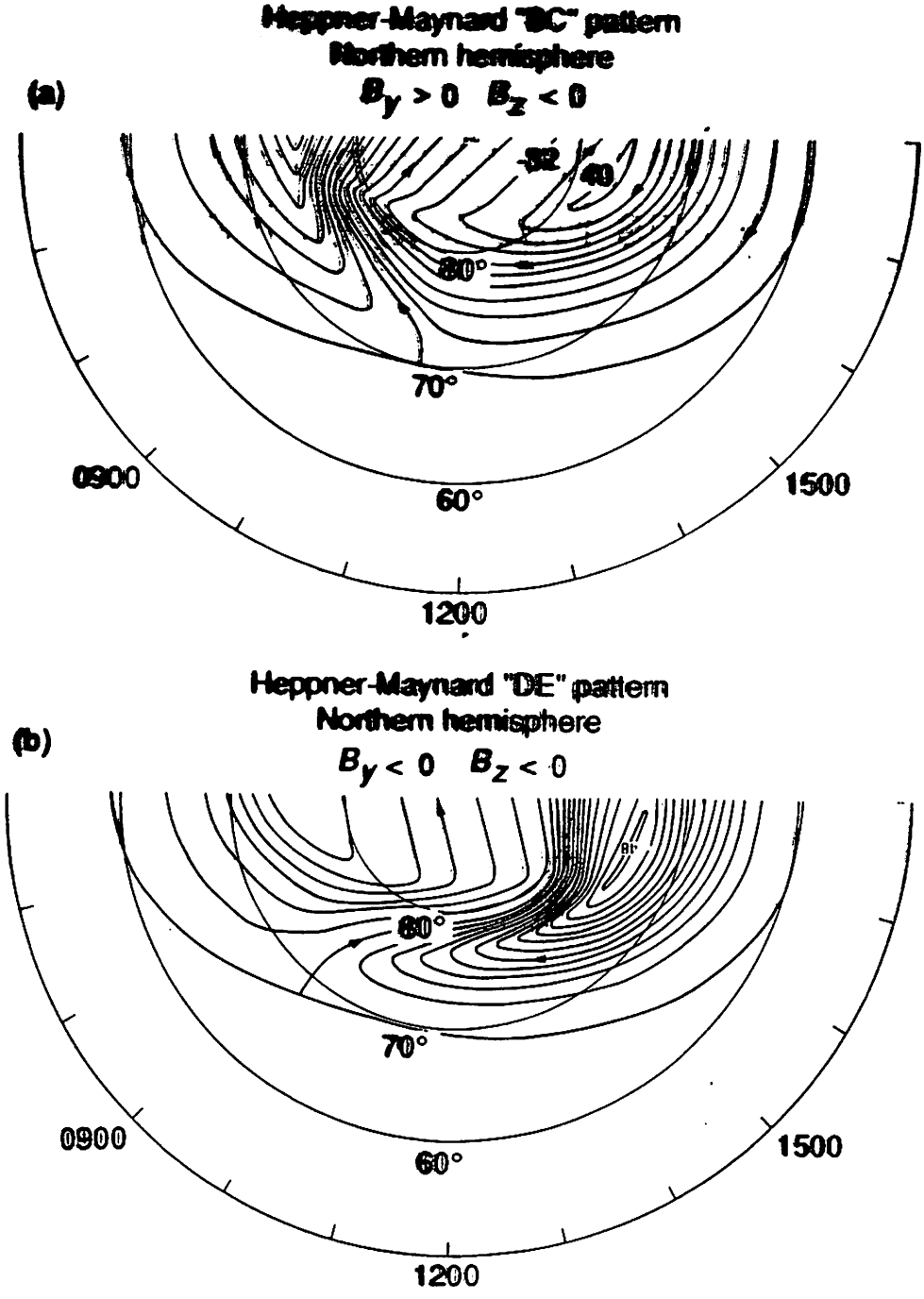
Heppner-Maynard "DC" pattern
Northern hemisphere
(a)
$B_y > 0$ $B_z < 0$
80°
70°
60°
0900
1500
1200
Heppner-Maynard "DE" pattern
Northern hemisphere
(b)
$B_y < 0$ $B_z < 0$
80°
70°
60°
0900
1500
1200

Fig. (1)

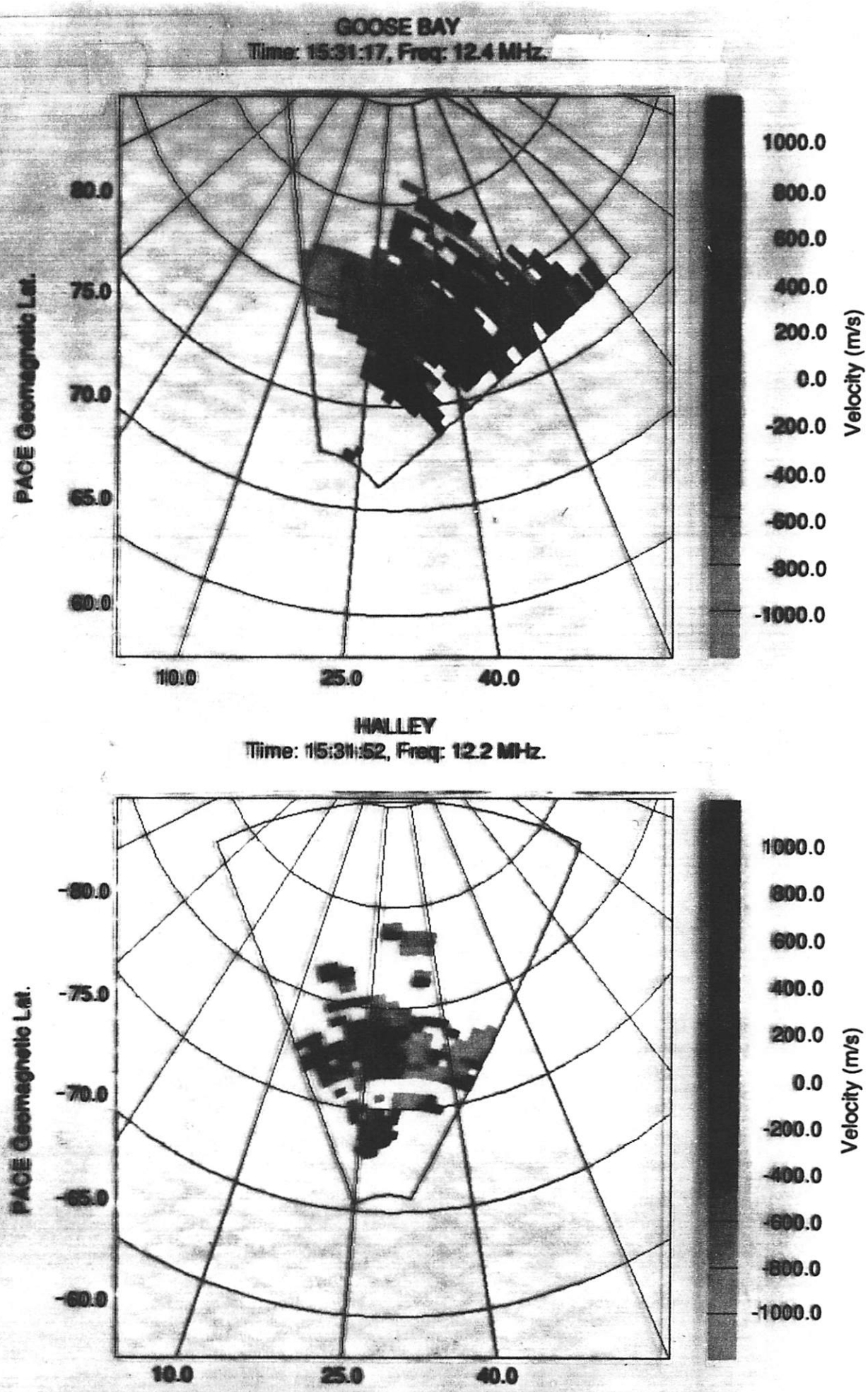

PACE Radar Comparison Plot 22/04/1988.

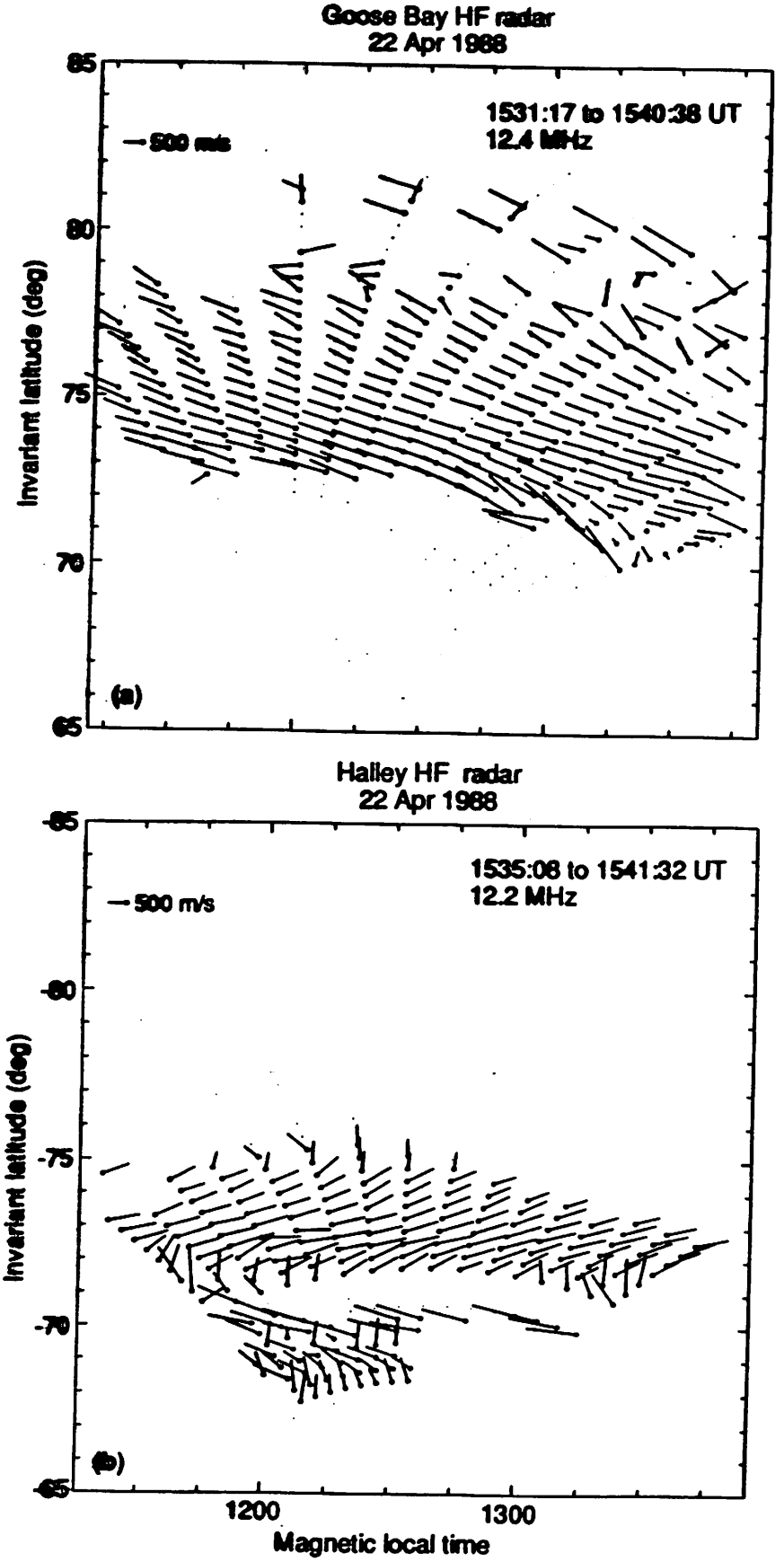
Goose Bay HF radar
22 Apr 1988
1531:17 to 1540:38 UT
12.4 MHz
500 m/s
Invariant latitude (deg)
85
80
75
70
65
(a)
Halley HF radar
22 Apr 1988
1535:08 to 1541:32 UT
12.2 MHz
500 m/s
-85
-80
-75
-70
-65
(b)
1200
1300
Magnetic local time

Fig. 6

THE JOHNS HOPKINS UNIVERSITY
PPLIED PHYSICS LABORATORY
LAUREL, MARYLAND

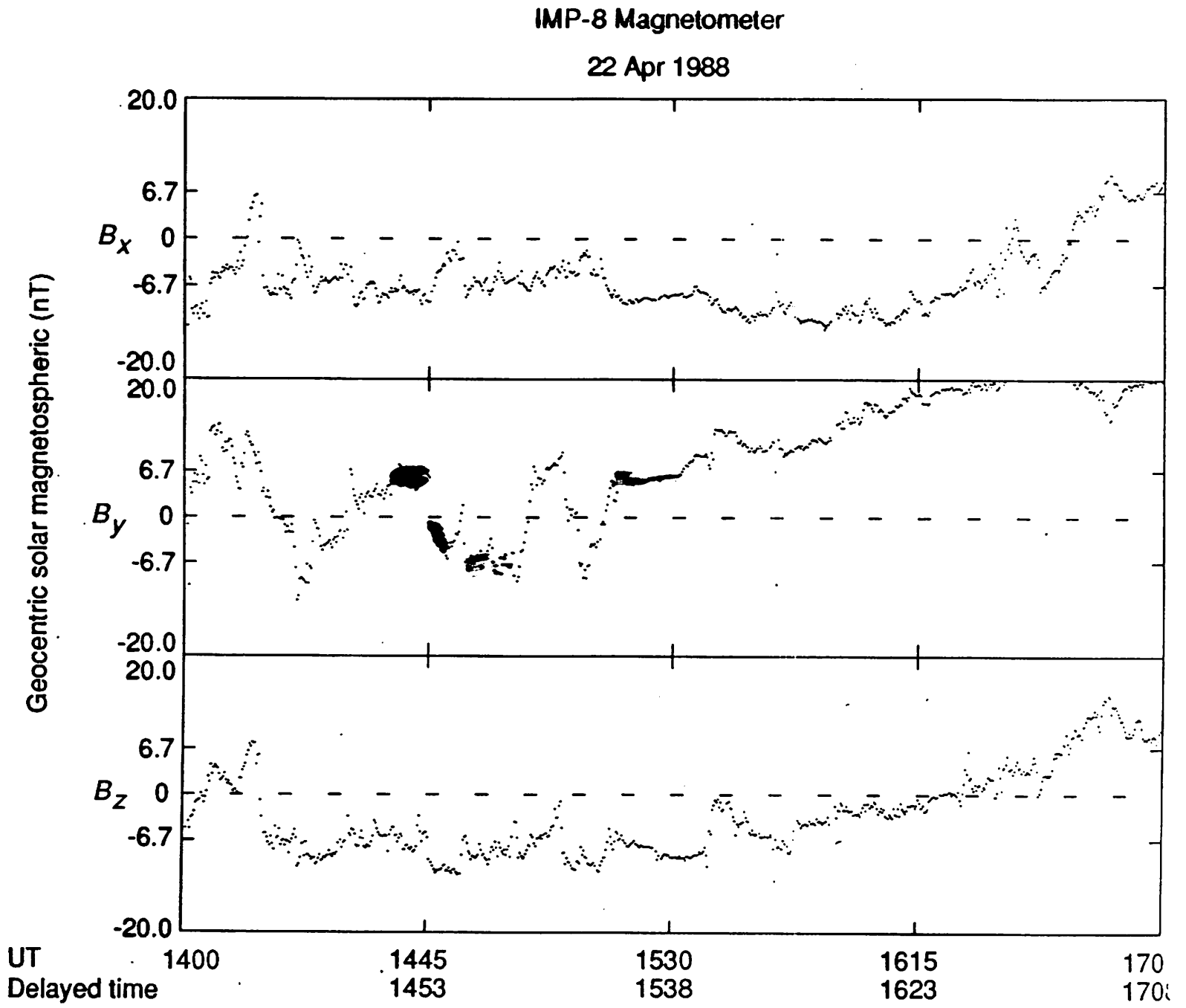

Fig. 3

THE JOHNS HOPKINS UNIVERSITY
APPLIED PHYSICS LABORATORY
LAUREL, MARYLAND

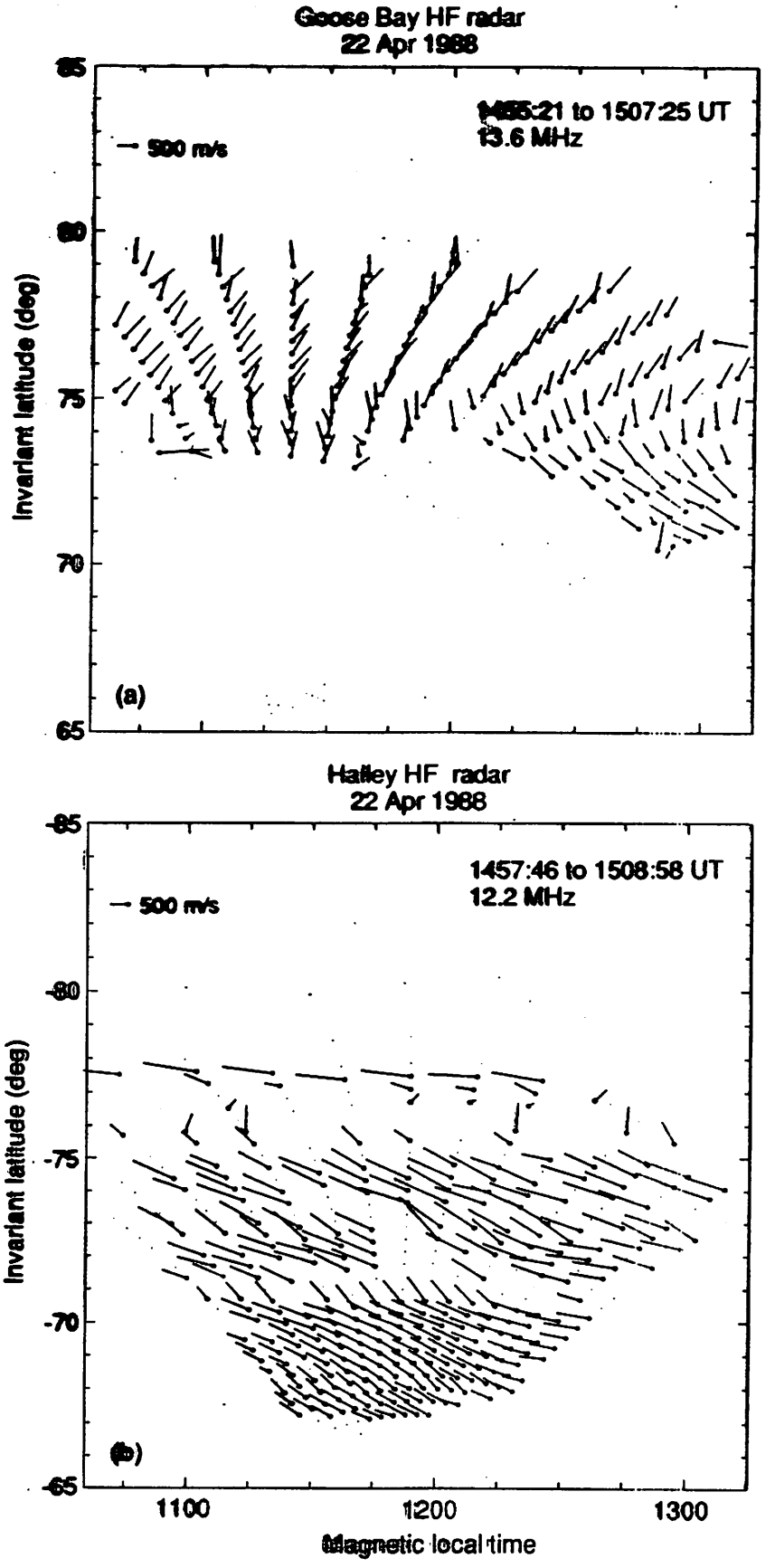

Fig. 7

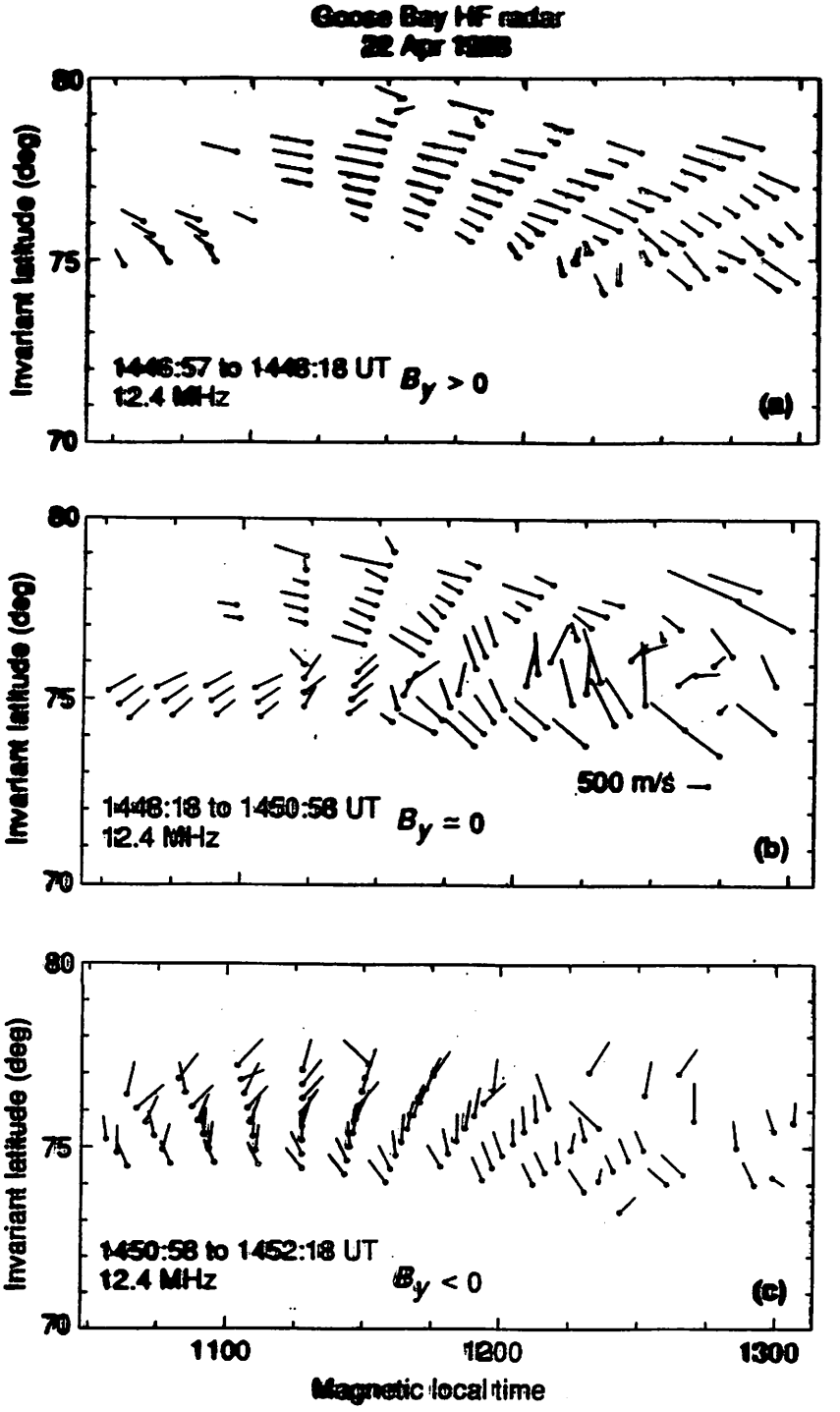

Fig. 9

The Johns Hopkins University
Applied Physics Laboratory
Geospace Remote Sensing

GRAVITY WAVES

MODELLING GRAVITY WAVE EFFECTS:

HF RAY TRACING

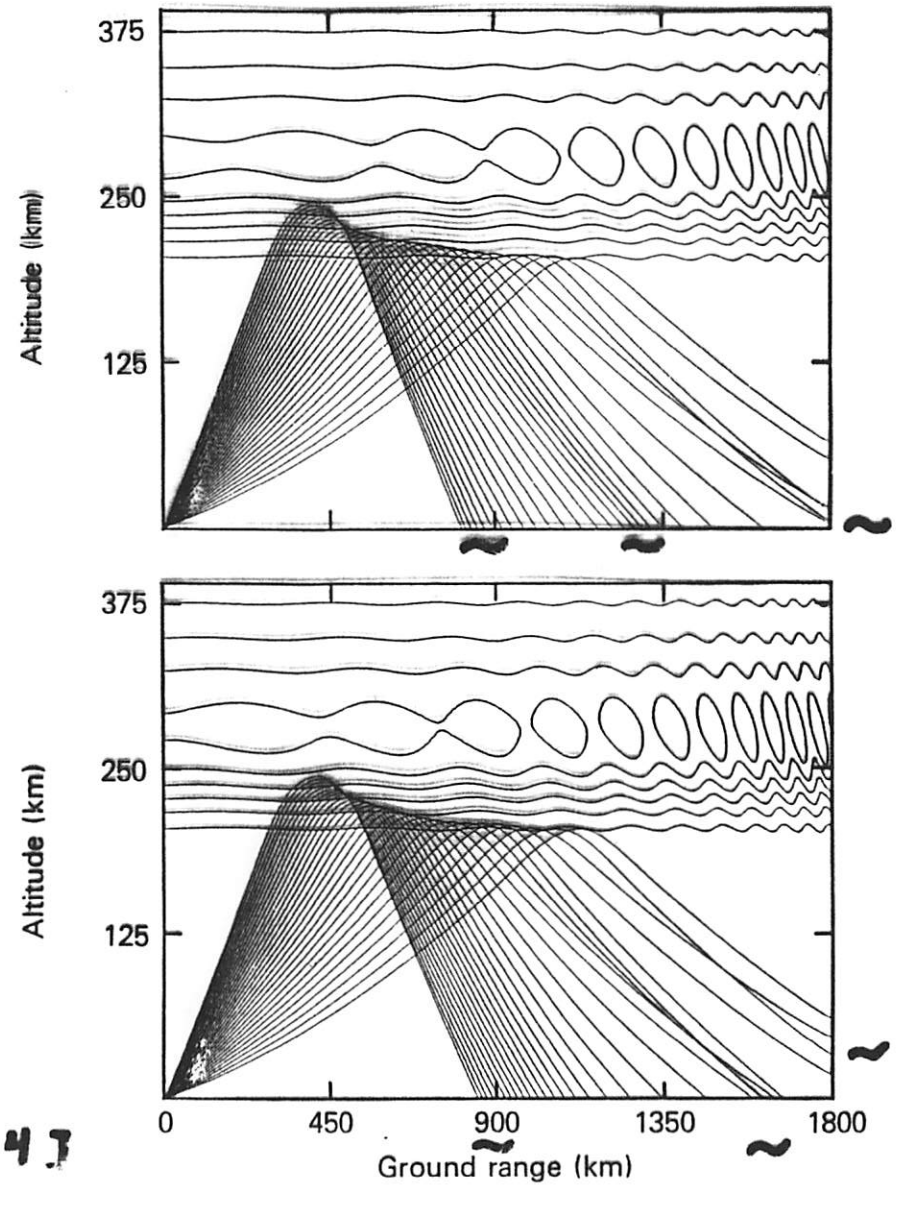

~ focusing

+ 15 MIN

TID due to Earth-Reflected Gravity Wave [Francis, JGR, 1974]

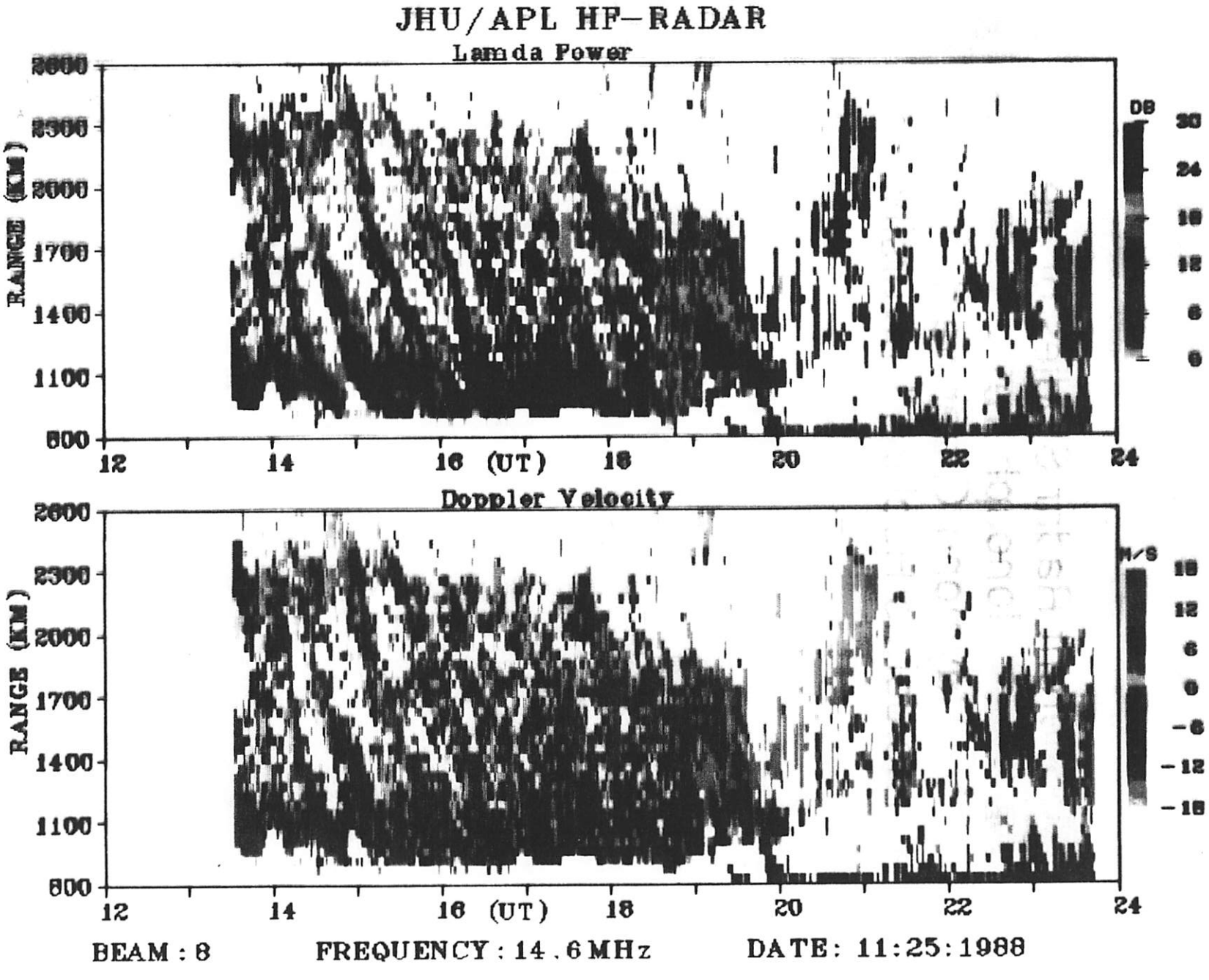
JHU/APL HF-RADAR
Lamda Power
RANGE (KM)
2600
2300
2000
1700
1400
1100
800
12
14
16 (UT)
18
20
22
24
DB
30
24
18
12
6
0
Doppler Velocity
RANGE (KM)
M/S
18
12
6
0
-6
-12
-18
BEAM : 8
FREQUENCY : 14.6 MHz
DATE: 11:25:1988

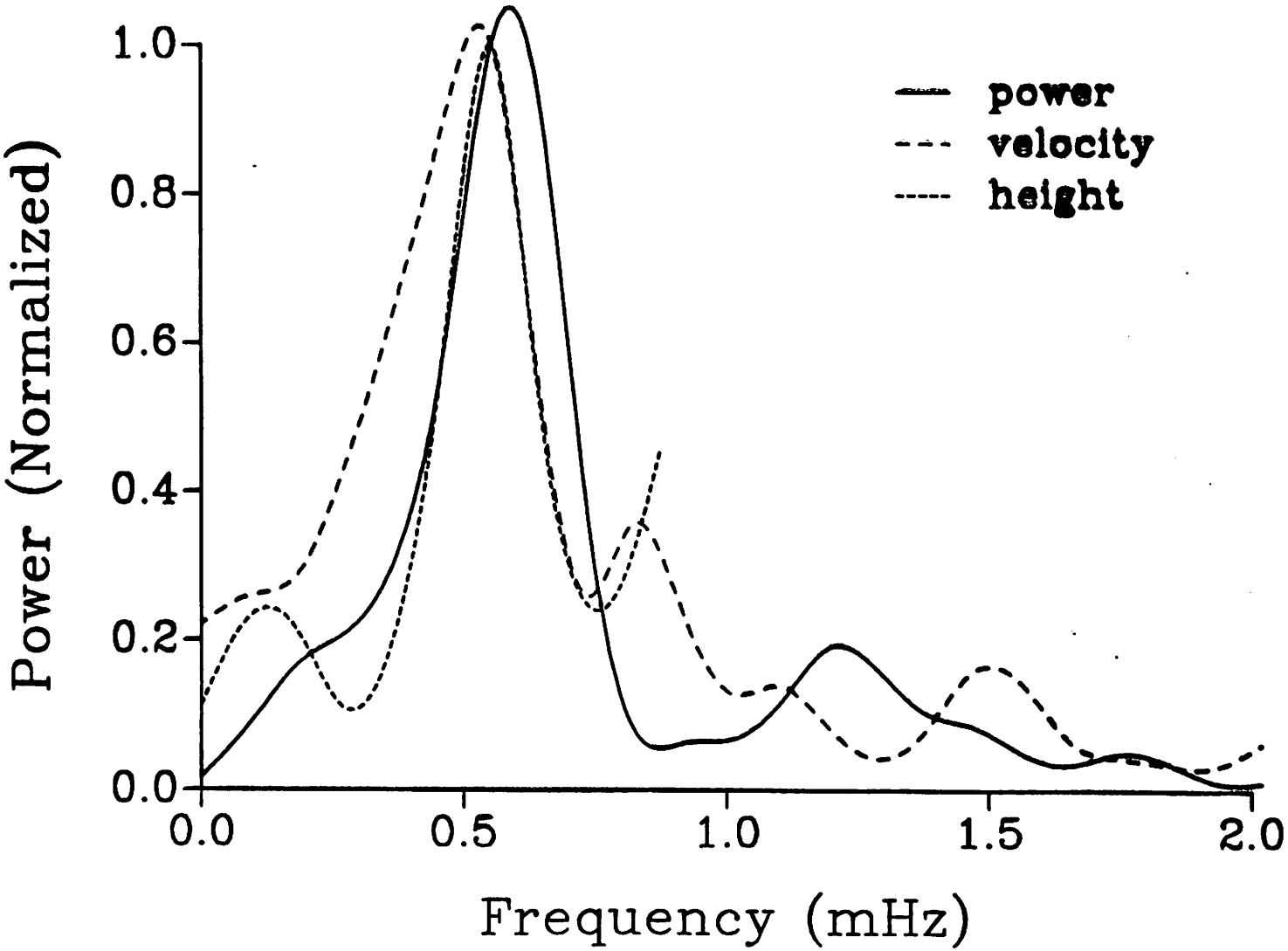
power
velocity
height
Power (Normalized)
1.0
0.8
0.6
0.4
0.2
0.0
0.0
0.5
1.0
1.5
2.0
Frequency (mHz)

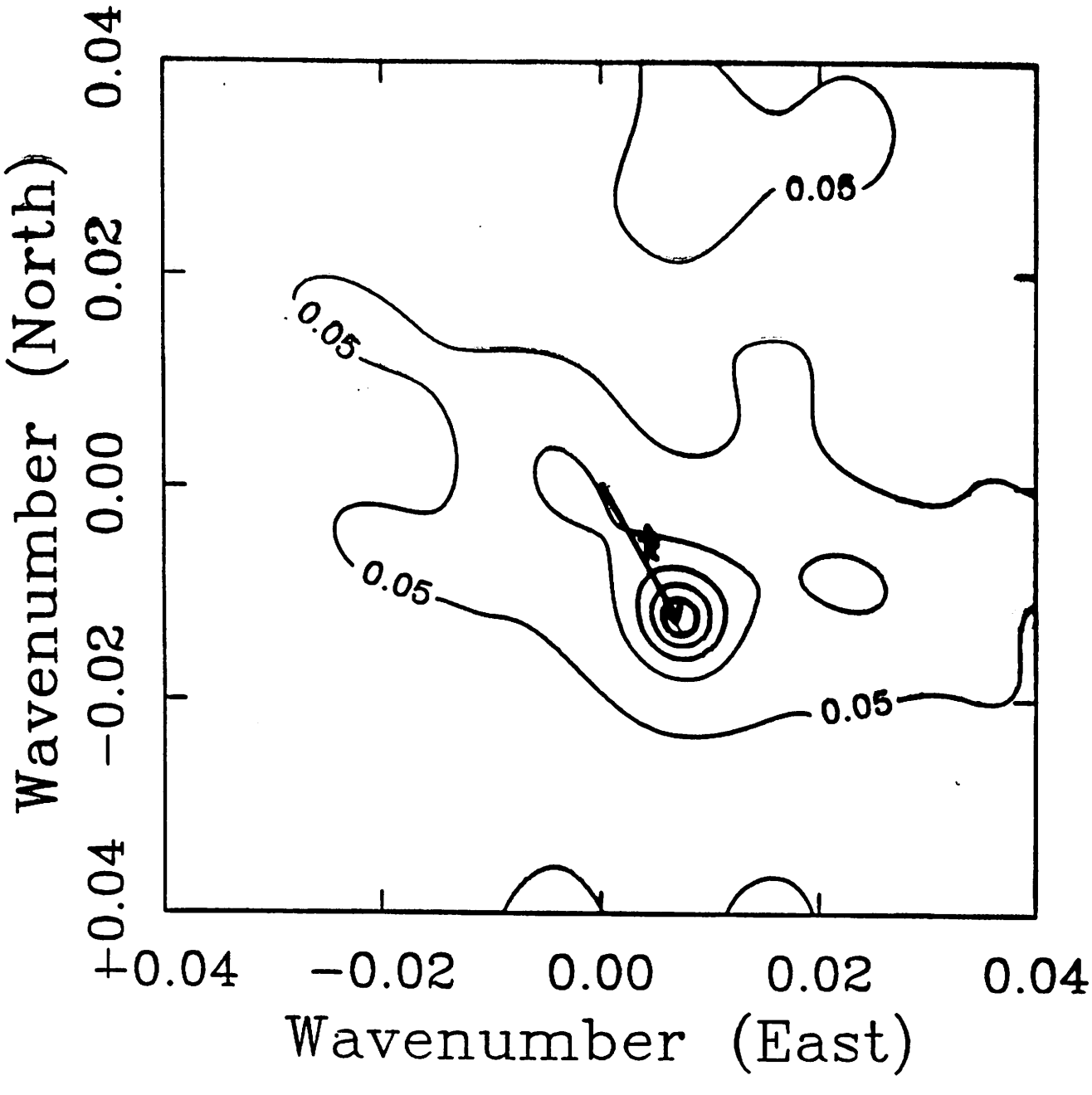
0.05
0.05
0.05
0.05
Wavenumber (North)
+0.04
−0.02
0.00
0.02
0.04
+0.04
−0.02
0.00
0.02
0.04
Wavenumber (East)

MODELLING GRAVITY WAVE PROPAGATION: THEORETICAL AND EXPERIMENTAL PHASE MAPS

NOVEMBER 25, 1988

ONSET:

~ 1211 UT

~ 2100 KM

BEAM 8

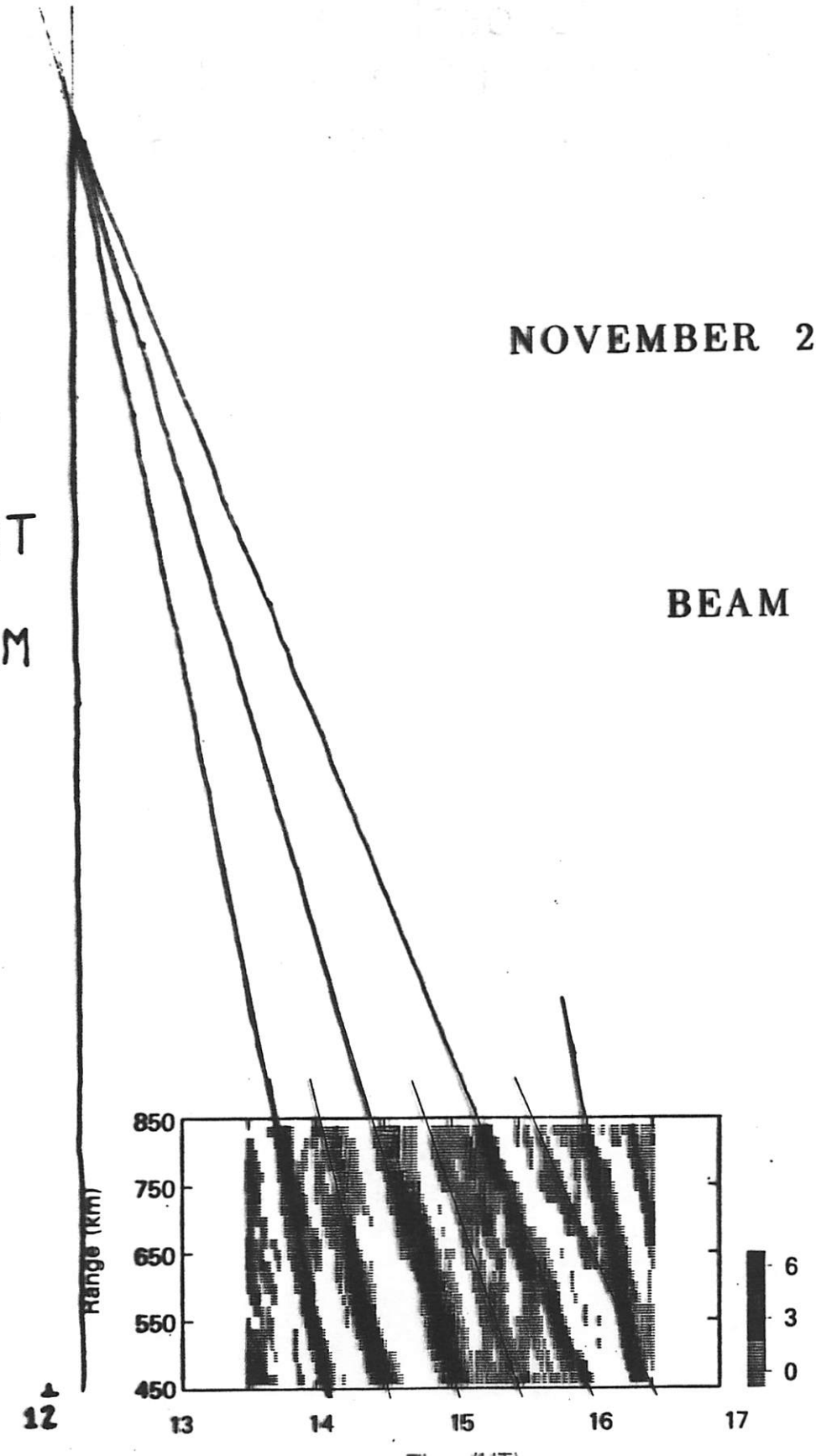

GENERATION OF A GRAVITY WAVE:
LATITUDINAL PROFILE OF CONVECTION VELOCITY

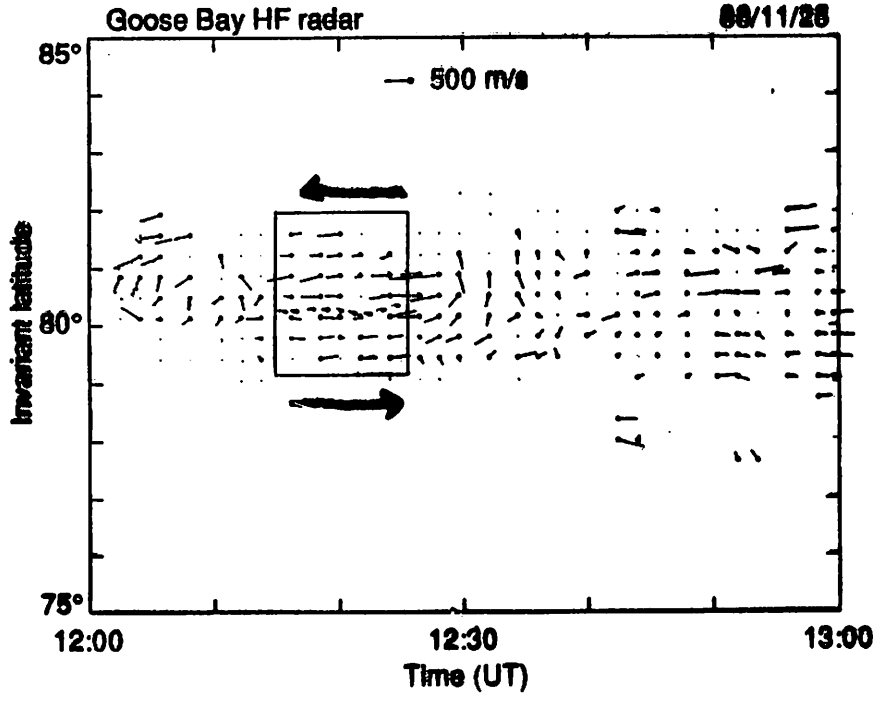

NOVEMBER 25, 1988 1200 — 1300 UT

SuperDARN

Global Imaging of Ionospheric dynamics

The Johns Hopkins University
Applied Physics Laboratory
Geospace Remote Sensing

What Is SuperDARN?

SuperDARN is an internationally-funded network of HF radars capable of continuous, global-scale observations of the high-latitude ionosphere.

The Johns Hopkins University
Applied Physics Laboratory
Geospace Remote Sensing

What is the basis of the SuperDARN concept?

Bidirectional common volume observations with pairs of HF radars to provide vector determinations of plasma convection and the ionospheric electric field

Spatial resolution of each vector

~50 km x ~50 km

Total spatial coverage

~40 million km^2

Observations will cover the auroral zone and polar cap

$65° < \Lambda < 85°$

~14 Hours of Magnetic Local Time

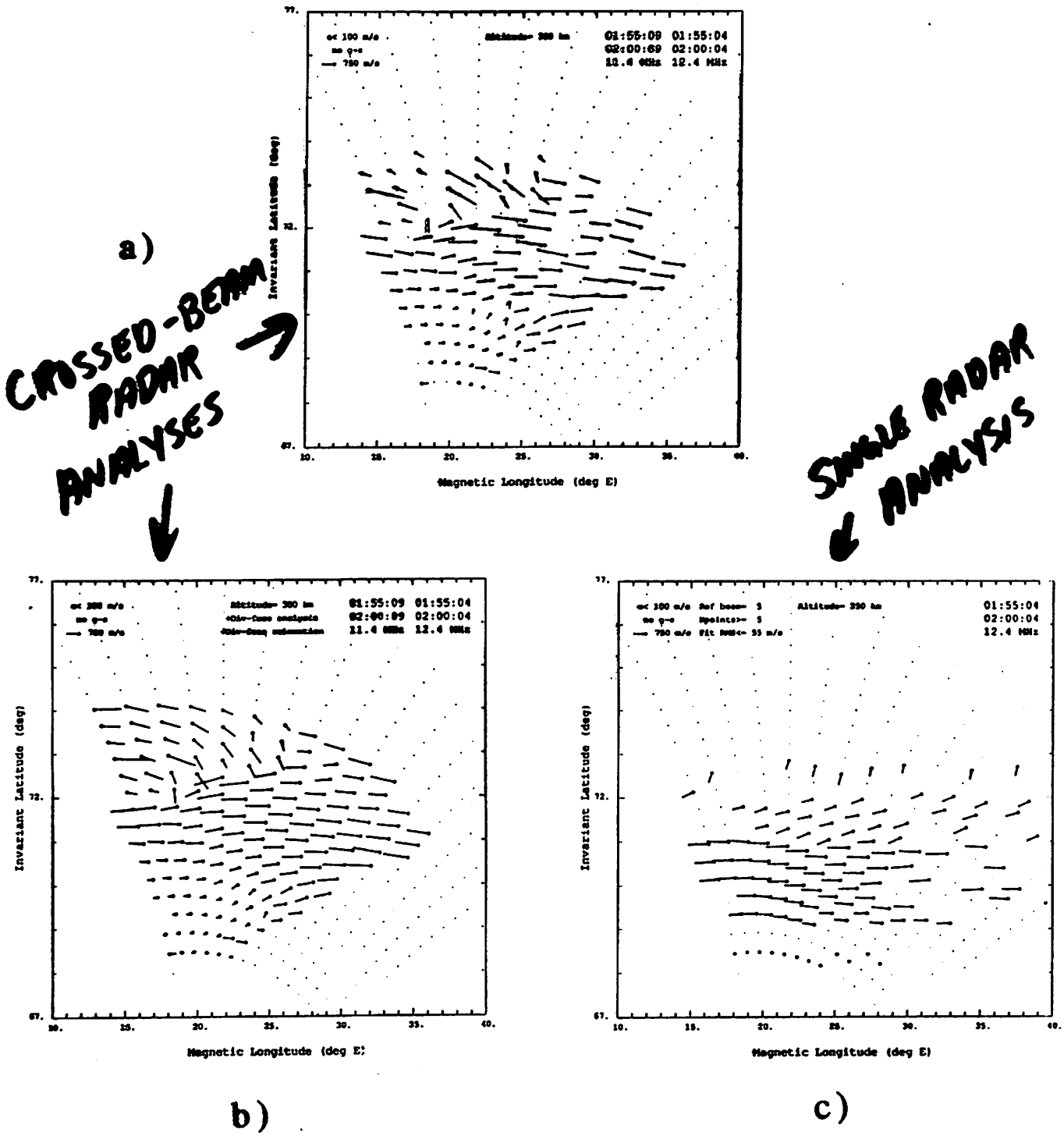

Figure 7 a) Map of convection velocity for the period December 6, 1989, 01:55 - 02:00 UT obtained by merging line of sight velocity data from the Goose Bay and Schefferville HF radars. b) Same as (a), except that the region of vector solution has been extended by applying the condition that the flow be free of divergence to Goose Bay line of sight data, followed by a relaxation of the overall pattern to a divergence-free state. c) Map of convection velocity for the period of (a) that is obtained by fitting the Goose Bay line of sight velocity data on the basis of an assumed L-shell invariance in the flow. Moderate fitting criteria have been applied.

The Johns Hopkins University
Applied Physics Laboratory
Geospace Remote Sensing

SuperDARN (Northern Hemisphere) Division of Responsibilities

Radar	Responsible Institutions	Status
Finland Iceland (East)	University of Leicester (UK)	Funded
Iceland (West)	CNRS/LCPE,CRPE,LSEET (France) JHU/APL (US)	Funded
Goose Bay (E.)	JHU/APL	Operational
Goose Bay (W.)	JHU/APL (US) CNRS/LCPE,CRPE,LSEET (France)	Funded
Saskatoon (E)	U. of Saskatoon (Canada) also: U. of Alberta U. of Western Ont. U. of Calgary York University	Funded

The Johns Hopkins University
Applied Physics Laboratory
Geospace Remote Sensing

SUPERDARN

Field-of-View Superimposed on Heppner-Maynard BC Pattern

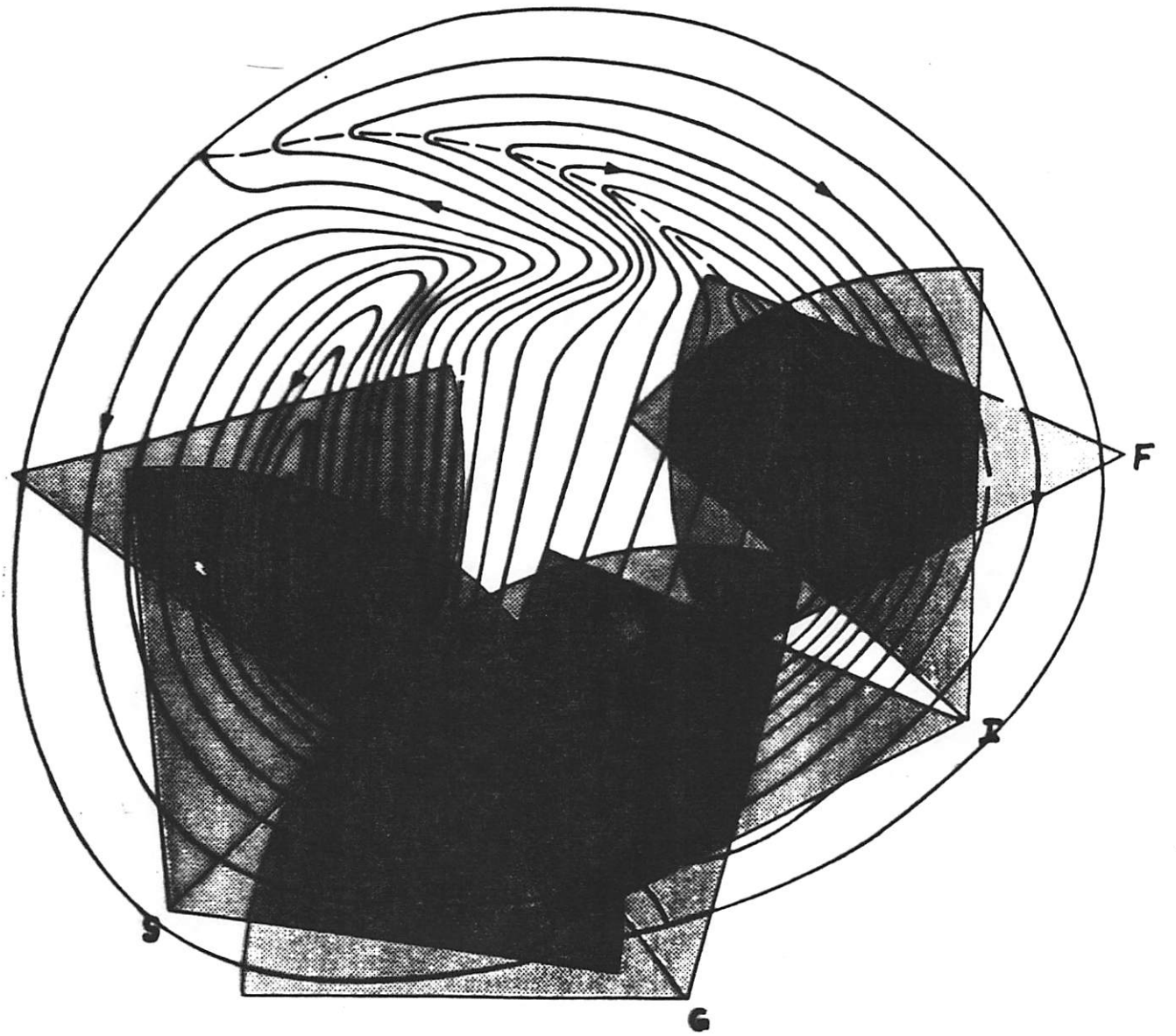

SuperDARN Data Flow

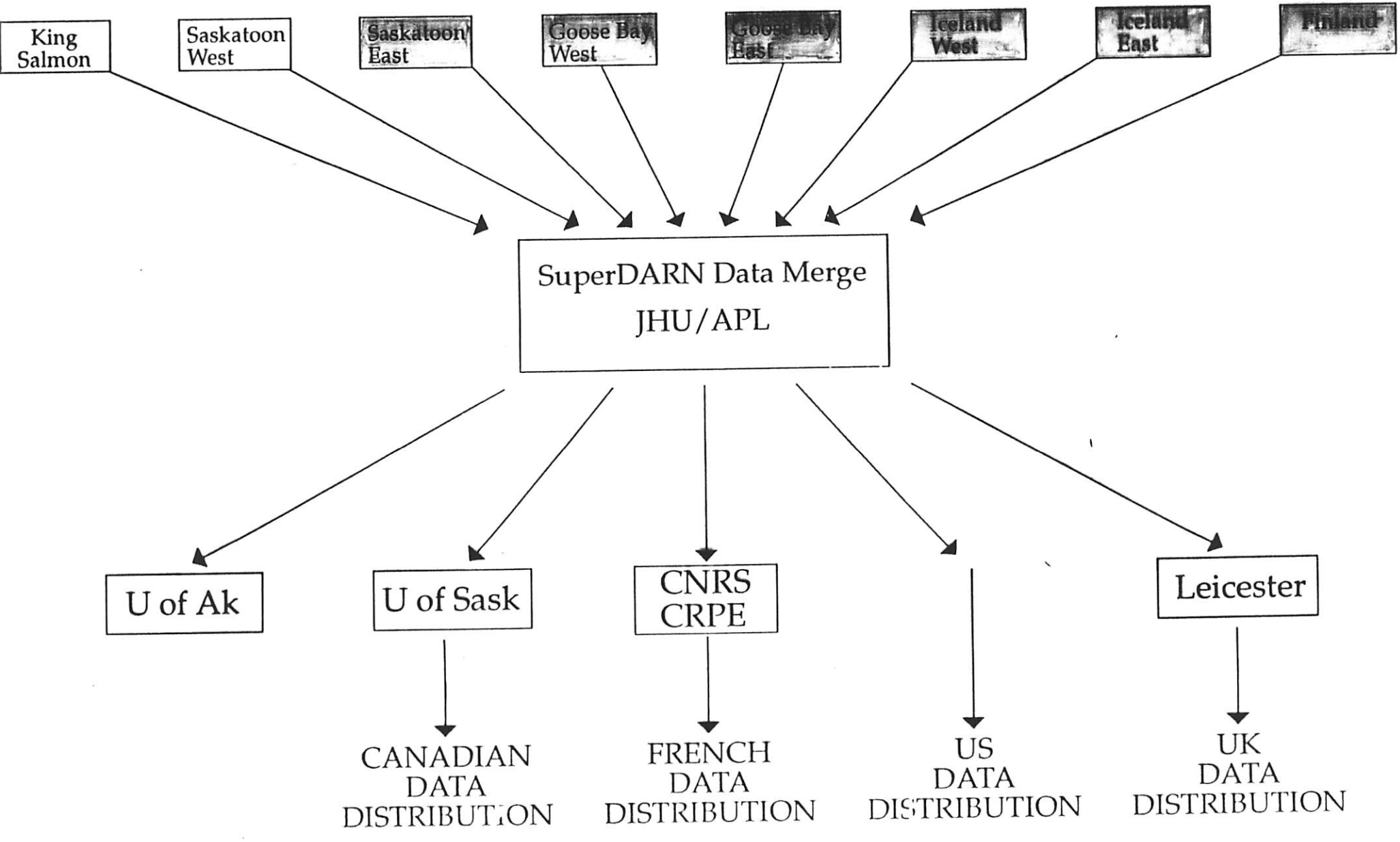

The Johns Hopkins University
Applied Physics Laboratory
Geospace Remote Sensing

Anticipated Contributions of SuperDARN to Solar-Terrestrial Research

- Data from SuperDARN will be shared by scientists in all participating countries
- Data from SuperDARN will be used to provide ground-based support to future multinational satellite missions including ISTP/GGS, CLUSTER, FREJA, and INTERBALL
- Data from SuperDARN will be used to support international scientific collaborations, e.g. STEP
- Data from SuperDARN will support national scientific initiatives, e.g. CEDAR, GEM

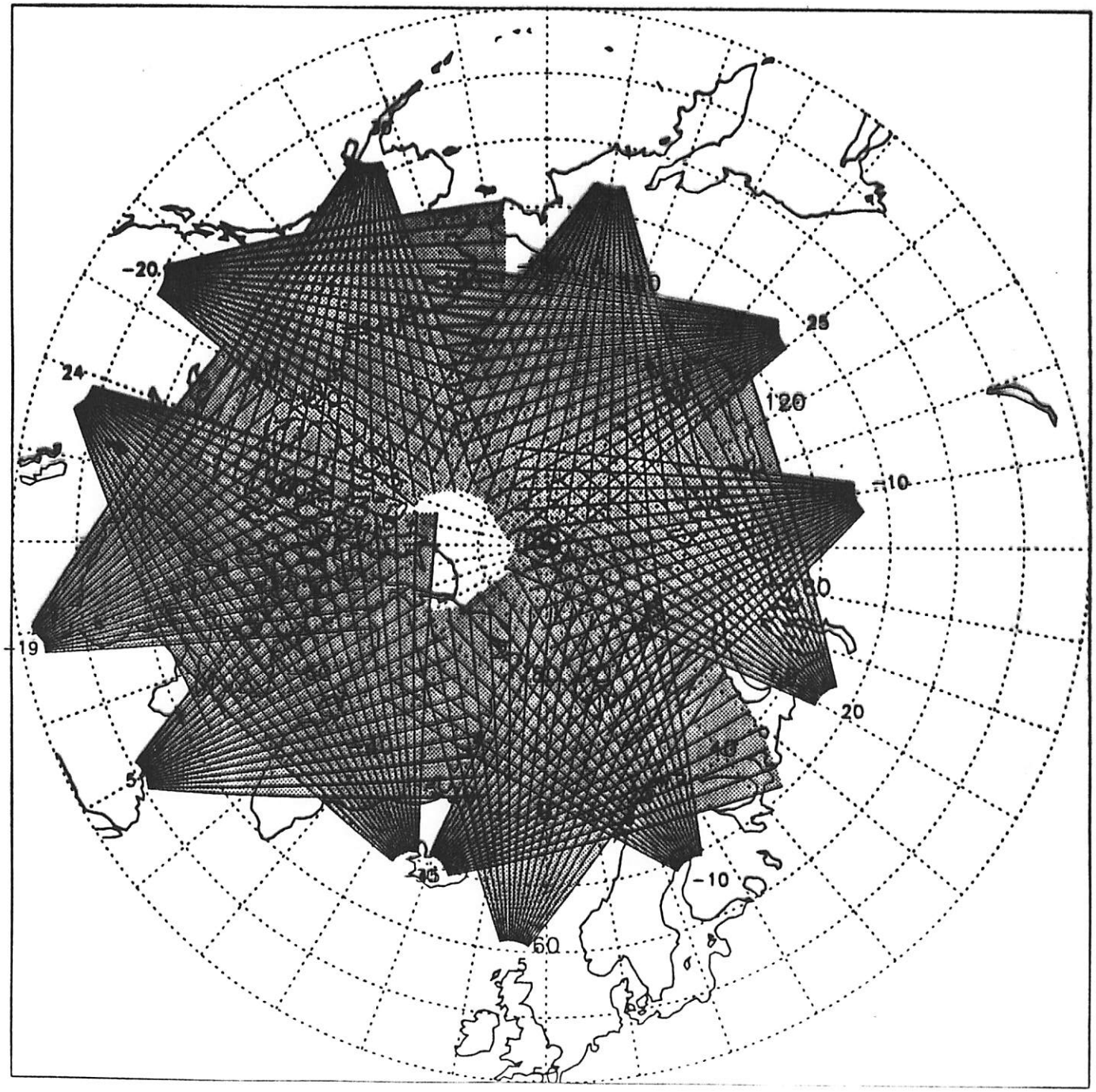
-20
24
25
120
-10
180
19
20
5
35
-10
50
5